Comparative Molecular Field Analysis of the Binding of the Stereoisomers of Fenoterol and Fenoterol Derivatives to the β_2 Adrenergic Receptor

Krzysztof Jozwiak,[†,‡] Chakir Khalid,[†,§] Mary J. Tanga,[||] Ilona Berzetei-Gurske,[||] Lucita Jimenez,[||] Joseph A. Kozocas,[||] Anthony Woo,[§] Weizhong Zhu,[§] Rui-Ping Xiao,[§] Darrell R. Abernethy,[⊥] and Irving W. Wainer*[,⊥]

Department of Chemistry, Medical University of Lublin, Lublin, Poland, Laboratory of Cardiovascular Science, National Institute on Aging Intramural Research Program, Baltimore, Maryland, SRI International, Menlo Park, California, and Laboratory of Clinical Investigation, National Institute on Aging Intramural Research Program, Baltimore, Maryland

Received January 9, 2007

Stereoisomers of fenoterol and six fenoterol derivatives have been synthesized and their binding affinities for the β_2 adrenergic receptor ($K_i\beta_2$-AR), the subtype selectivity relative to the β_1-AR ($K_i\beta_1$-AR/$K_i\beta_2$-AR) and their functional activities were determined. Of the 26 compounds synthesized in the study, submicromolar binding affinities were observed for (*R*,*R*)-fenoterol, the (*R*,*R*)-isomer of the *p*-methoxy, and (*R*,*R*)- and (*R*,*S*)-isomers of 1-naphthyl derivatives and all of these compounds were active at submicromolar concentrations in cardiomyocyte contractility tests. The $K_i\beta_1$-AR/$K_i\beta_2$-AR ratios were >40 for (*R*,*R*)-fenoterol and the (*R*,*R*)-*p*-methoxy and (*R*,*S*)-1-naphthyl derivatives and 14 for the (*R*,*R*)-1-napthyl derivative. The binding data was analyzed using comparative molecular field analysis (CoMFA), and the resulting model indicated that the fenoterol derivatives interacted with two separate binding sites and one steric restricted site on the pseudo-receptor and that the chirality of the second stereogenic center affected $K_i\beta_2$ and subtype selectivity.

Introduction

Fenoterol, 5-[1-hydroxy-2-[[2-(4-hydroxyphenyl)-1-methylethyl]-amino]ethyl]-1,3-benzenediol (Figure 1, compound **1**) is a β_2-adrenoceptor (β_2-AR) agonist,[1] which exists as four stereoisomers. The clinically used drug, *rac*-fenoterol, is a racemic mixture of (*R*,*R*)-**1** and (*S*,*S*)-**1**, and this mixture is used for the treatment of asthma[2] and may also be useful in the treatment of congestive heart failure.[3,4]

Initial ligand displacement binding studies using (*R*,*R*)-**1** and (*S*,*S*)-**1** were carried out using rat erythrocytes. The data demonstrated that (*R*,*R*)-**1** displaced the marker ligand [^{3}H]-dihydroalprenolol with a K_d of 2.88×10^{-6} M, *rac*-**1** had a K_d of 5.79×10^{-5} M, and (*S*,*S*)-**1** had no measurable specific binding.[5] The enantioselectivity of the β_2-AR binding was recently confirmed.[6] In the latter study, (*R*,*R*)-**1** and (*S*,*S*)-**1** were prepared using an amylose tris-(3,5-dimethylphenylcarbamate) chiral stationary phase, and the binding studies were conducted using membranes from HEK-293 cells that express human β_2-AR. The calculated K_d for (*R*,*R*)-**1** was 460 nM and the K_d for (*S*,*S*)-**1** was >100 000 nM.

The pharmacological effects of (*R*,*R*)-**1** and (*S*,*S*)-**1** were also examined in the latter study using cardiomyocyte contractility in freshly isolated adult rat cardiomyocytes.[6] In this model, (*R*,*R*)-**1** increased the maximum contractile response from 265 ± 11.6% to 306 ± 11.8% of resting cell length ($P < 0.05$) and reduced EC_{50} from −7.0 ± 0.27 log [M] to −7.1 ± 0.20 log [M], while (*S*,*S*)-**1** had no significant effect.

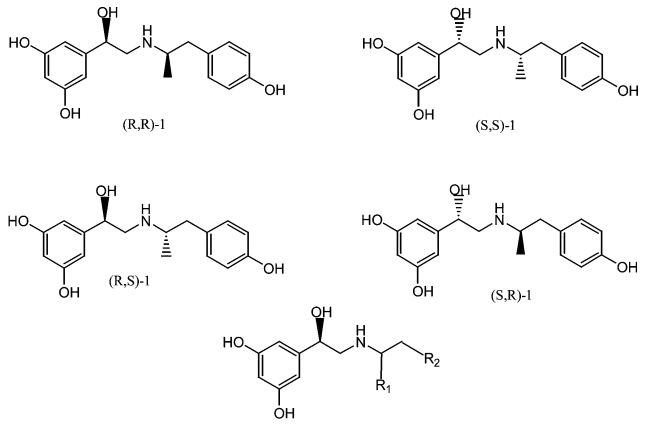

Compounds	R1	R2
2	CH_3	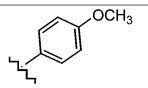
3	CH_3	
4	CH_3	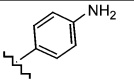
5	CH_3	
6	CH_3	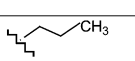
7	H	

Figure 1. The structures of the stereoisomers of fenoterol and the compounds **2**−**7** that were synthesized in this study.

While the binding affinities and pharmacological effects of (*R*,*R*)-**1** and (*S*,*S*)-**1** have been examined, to our knowledge there have been no similar studies of (*R*,*S*)-**1** and (*S*,*R*)-**1**. Therefore,

* To whom correspondence should be addressed. Irving W. Wainer, National Institute on Aging, National Institutes of Health Gerontology Research Center, 5600 Nathan Shock Drive, Baltimore, MD 21224-6825. Phone: (410)-558-8498. Fax: (410)-558-8409. E-mail: wainerir@grc.nia.nih.gov.

† Equal contributors.

‡ Medical University of Lublin.

§ Laboratory of Cardiovascular Science, National Institute on Aging Intramural Research Program.

|| SRI International.

⊥ Laboratory of Clinical Investigation, National Institute on Aging Intramural Research Program.

10.1021/jm070030d CCC: $37.00
Published on Web 05/17/2007

Scheme 1

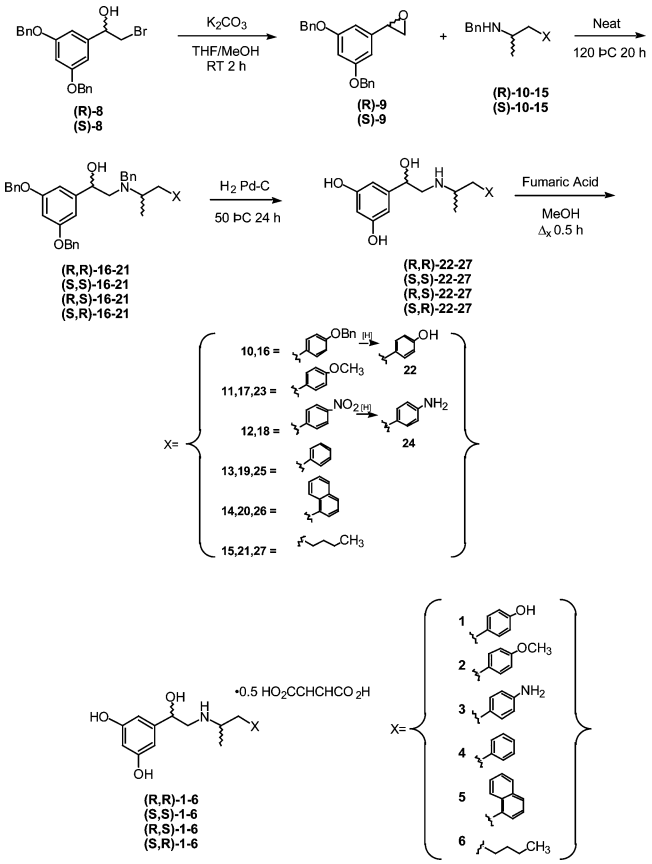

the objectives of this study were to develop a synthetic approach for the preparation of (*R*,*S*)-**1** and (*S*,*R*)-**1** and to determine their respective binding affinities and pharmacological effects. In addition, the study was designed to synthesize and characterize a series of derivatives of **1**, compounds **2**−**7** (Figure 1), to determine the effect of altering the 4-hydroxyphenyl moiety and the removing of the second chiral center. The aim of the project was the development of a pharmacophore model, which could be used as a structural guide for the design of new compounds with β_2-AR selectivity which can be tested for use in the treatment of congestive heart failure.

Synthetic Approach. The key step in the synthesis of the four stereoisomers of **1**−**6** was the coupling of the epoxide formed from either (*R*)- or (*S*)-3′,5′-dibenzyloxyphenylbromohydrin with the (*R*)- or (*S*)-enantiomer of the appropriate benzyl-protected 2-amino-3-benzylpropane (**1**−**5**) or the (*R*)- or (*S*)-enantiomer of *N*-benzyl-2-aminoheptane (**6**), Scheme 1. The synthesis of (*R*)-**7** and (*S*)-**7** was accomplished using 2-phenethylamine, Scheme 2. This approach was similar to the one developed by Trofast et al.[7] for the synthesis of the stereoisomers of formoterol, compound **47**, Figure 2. The resulting compounds were then deprotected by hydrogenation over Pd/C and purified as the fumarate salts.

The chiral building blocks used in the syntheses were produced using Scheme 3. The (*R*)- and (*S*)-3′,5′-dibenzyloxyphenyl-bromohydrin enantiomers were obtained by the enantiospecific reduction of 3,5-dibenzyloxy-α-bromoacetophenone using boron-methyl sulfide complex (BH_3SCH_3) and either (1*R*,2*S*)- or (1*S*,2*R*)-*cis*-1-amino-2-indanol. The required (*R*)- and (*S*)-2-benzylaminopropanes were prepared by enantioselective crystallization of the *rac*-2-benzylaminopropanes using either (*R*)- or (*S*)-mandelic acid as the counterion.

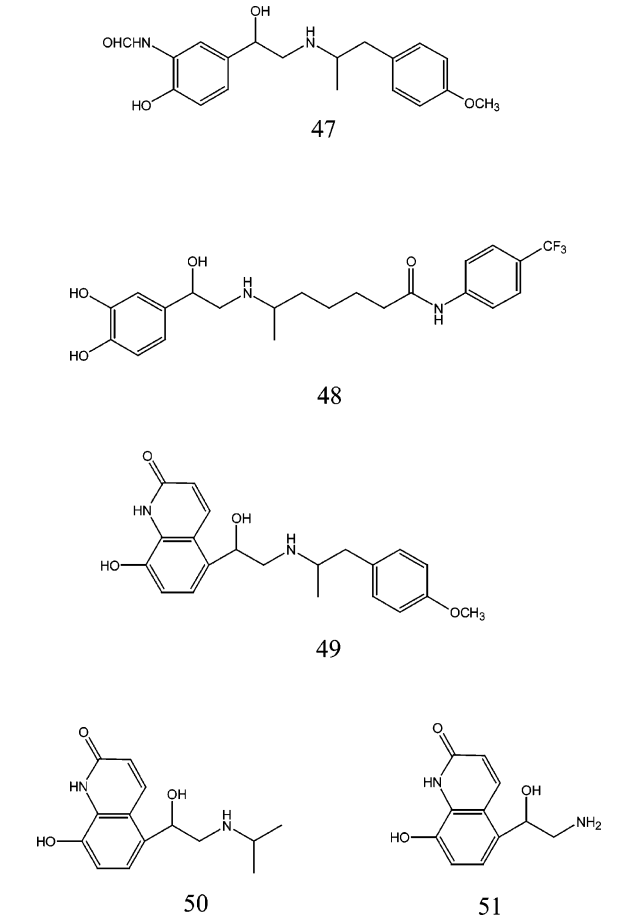

Figure 2. The structures of compounds **47**−**51**.

Scheme 2

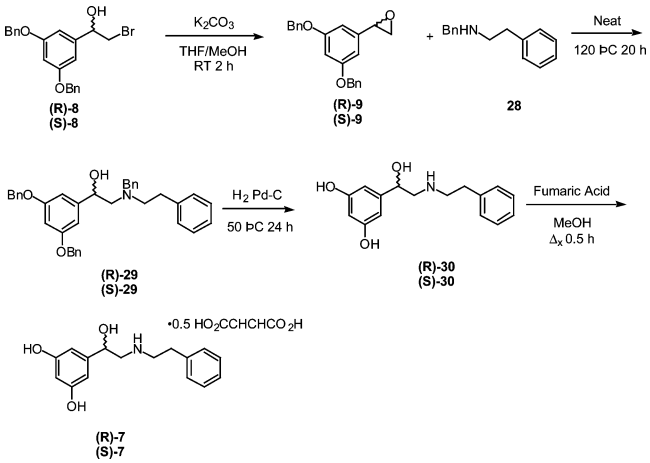

Results

Membrane Binding Studies. Binding affinities, expressed as K_i values, were determined using membranes obtained from a HEK 293 cell line stably transfected with cDNA encoding human β_2-AR[8] with [^{3}H]CGP-12177 as the marker ligand. The resulting IC_{50} values and Hill coefficients were calculated for each test compound using Prism software and K_i values were calculated using the Cheng−Prusoff transformation[9]

$$K_i = IC_{50}/(1 + L/K_d) \quad (1)$$

where L is the concentration of [^{3}H]CGP-12177 and K_d is the binding affinity of the [^{3}H]CGP-12177. Each test compound was assayed three times.

Scheme 3

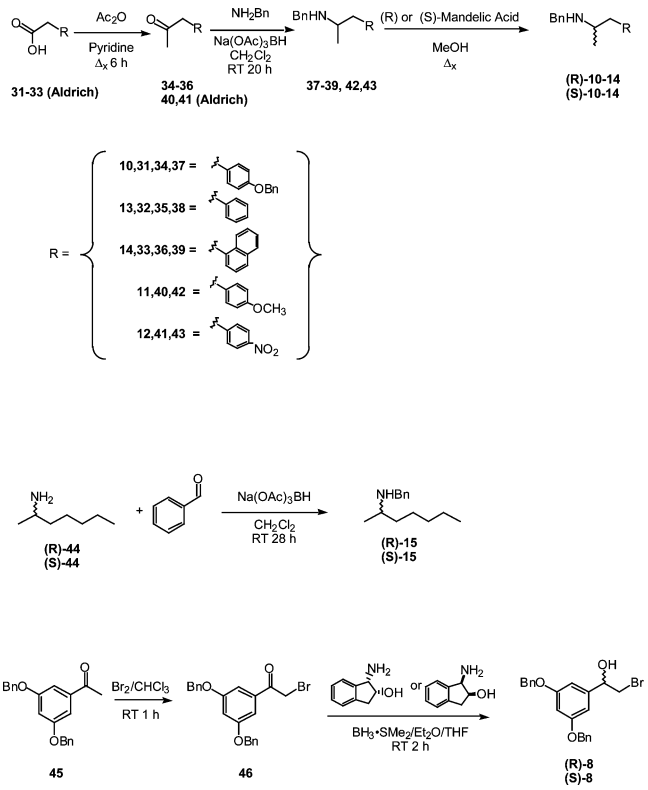

Table 1. Binding Affinities to the β_2-AR of the Compounds Synthesized in this Study Calculated as $K_i \pm$ SEM (μM), $n = 3$. Comparison of β_1- and β_2-Adrenergic Binding Affinity of Fenoterol Isomers

cmpd	$K_i\beta_1$	$K_i\beta_2$	$K_i\beta_1/K_i\beta_2$
(*R*,*R*)-**1**	14.8 ± 2.5	0.35 ± 0.03	43
(*R*,*S*)-**1**	18.9 ± 2.4	3.69 ± 0.25	5
(*S*,*R*)-**1**	>100	10.3 ± 1.4	NC
(*S*,*S*)-**1**	>100	27.8 ± 6.8	NC
(*R*,*R*)-**2**	21.9 ± 3.1	0.47 ± 0.04	46
(*R*,*S*)-**2**	30.8 ± 6.5	1.93 ± 0.14	16
(*S*,*R*)-**2**	33.4 ± 9.2	5.27 ± 0.51	6
(*S*,*S*)-**2**	>100	15.9 ± 2.7	NC
(*R*,*R*)-**3**	24.9 ± 2.1	2.93 ± 0.17	9
(*R*,*S*)-**3**	31.3 ± 3.5	7.94 ± 0.39	4
(*S*,*R*)-**3**	77.5 ± 3.6	23.1 ± 2.1	3
(*S*,*S*)-**3**	31.4 ± 1.7	28.6 ± 0.9	1
(*R*,*R*)-**4**	17.2 ± 1.3	1.86 ± 0.18	9
(*R*,*S*)-**4**	33.1 ± 2.8	6.04 ± 0.43	4
(*S*,*R*)-**4**	>100	30.8 ± 3.3	NC
(*S*,*S*)-**4**	>100	28.8 ± 1.8	NC
(*R*,*R*)-**5**	3.35 ± 0.13	0.24 ± 0.04	14
(*R*,*S*)-**5**	15.8 ± 6.3	0.34 ± 0.02	46
(*S*,*R*)-**5**	34.7 ± 9.1	1.78 ± 0.15	19
(*S*,*S*)-**5**	>100	2.54 ± 0.21	NC
(*R*,*R*)-**6**	10.2 ± 0.5	9.28 ± 0.90	1
(*R*,*S*)-**6**	>100	31.4 ± 1.7	NC
(*S*,*R*)-**6**	61.3 ± 5.8	>100	NC
(*S*,*S*)-**6**	52.6 ± 1.4	56.42 ± 5.19	1
(*R*) -**7**	42.5 ± 3.5	10.5 ± 1.5	4
(*S*)-**7**	52.2 ± 3.0	20.6 ± 3.7	3

The relative binding affinities to the β_2-AR for the stereoisomers of compounds **1**−**4** and **6** were *R*,*R* > *R*,*S* > *S*,*R* ≈ *S*,*S* (Table 1). This stereoselectivity is consistent with the previously reported potencies of the formoterol stereoisomers[7] and results from binding studies with the isoproterenol derivative PTFAM, compound **48**, Figure 2.[10] With compound **5**, no significant difference was found between the K_d values of the *R*,*R*- and *R*,*S*-isomers, thus, the order was *R*,*R* = *R*,*S* > *S*,*R* > *S*,*S*. The K_d value for (*R*)-**7** was greater than that of (*S*)-**7**, which is consistent with the established enantioselective binding preference for β_2-ARs, with the *R*-configuration at the stereogenic center containing the β-OH moiety, compare refs 10−13.

When just the *R*,*R*-isomers were compared, (*R*,*R*)-**5** had the highest relative affinity of the tested compounds, although the difference between (*R*,*R*)-**5** and (*R*,*R*)-**1** did not reach statistical significance, Table 1. The only other (*R*,*R*)-stereoisomer with submicromolar affinity was (*R*,*R*)-**2**, which had a significantly lower binding affinity than (*R*,*R*)-**5**, $p = 0.0051$, and (*R*,*R*)-**1**, $p = 0.0291$, although the mean K_d value for (*R*,*R*)-**2** is only 23% greater than that of (*R*,*R*)-**1**. The minimal effect of transforming the *p*-OH moiety into a methyl ether is consistent with previous data from Schirrmacher et al.[14] In the previous study, *rac*-**1** was converted into a [^{18}F]-fluoroethoxy ether without significant loss of in vitro activity, and the authors concluded that, within the accuracy of the experimental measurements, the derivatization did not change the binding affinity of the *rac*-**1** to the β_2-AR.

Binding affinities, expressed as K_i values, for the β_1-AR were determined using rat cortical membranes, with [^{3}H]-CGP-12177 as the marker ligand.[15] The calculated K_i for (*R*,*R*)-**5** was 3.35 μM and the binding affinities for the all of the remaining test compounds were >100 μM, Table 1. Unlike the data from the β_2-AR binding studies, there was no clear trend that could be associated with the stereochemistry of the compounds.

The relative selectivity of the compounds for the β_2-AR and β_1-AR was determined using the ratio $K_i\beta_1/K_i\beta_2$, Table 1. Of particular interest were the ratios for the four compounds with submicromolar affinity for the β_2-AR, (*R*,*R*)-**1**, (*R*,*R*)-**2**, (*R*,*R*)-**5**, and (*R*,*S*)-**5**, which were 46, 43, 14, and 46, respectively. The results for (*R*,*R*)-**1** and (*R*,*R*)-**2** are consistent with the previously reported $K_i\beta_1/K_i\beta_2$ ratio of 53 for the β_2-AR-selective agonist (*R*,*R*)-TA-2005, compound **49**, Figure 2.

The observed loss of β_2-AR selectivity for (*R*,*R*)-**5** was unexpected, as was the 3-fold increase in selectivity displayed by (*R*,*S*)-**5** relative to (*R*,*R*)-**5**. Previous studies with the stereoisomers of **47** indicated that both the (*R*,*R*)-isomer and the (*R*,*S*)-isomer had a high degree of selectivity for the β_2-AR relative to the β_1-AR, with the selectivity of the (*R*,*R*)-isomer greater than that of the (*R*,*S*)-isomer.[7] This is the case for compounds **1** and **2**, but reversed for **5**. It is also interesting to note that (*S*,*R*)-**5** had a similar selectivity (19-fold) and its affinity for the β_2-AR was only 7-fold weaker than (R,R)-**5**, 1.78 μM and 0.24 μM, respectively.

Cardiomyocyte Contractility. The pharmacological activities of the compounds with submicromolar affinity for the β_2-AR and (*R*,*S*)-**1** and (*S*,*S*)-**1** were assessed using cardiomyocyte contractility, as previously described.[6] In these studies, the contraction amplitude indexed by electrical pacing induced shortening of cell length was measured in single ventricular myocytes before and after exposure to a single dose of the test compounds. Contractile response to the agonist was expressed as a percentage of the basal contractility, and the specificity of the agonist toward β_2-adrenergic receptor was determined by the inhibitory effect of ICI 118 551 (10^{-7} mol/L), a selective β_2-AR antagonist.

All of the compounds tested, except for (*S*,*S*)-**1**, produced a significant contractile response, which was blocked by ICI 118 551, while (*S*,*S*)-**1** had no observed pharmacological effect, Figure 3. These results were consistent with the results from the previous study[6] and with the observations that for agonist activity at the β_2-AR an *R*-configuration is preferred at the stereogenic center containing the β-OH moiety, compare refs 10−13. It is of interest to note that maximum effect was elicited with 0.1 μM (*R*,*R*)-**5** and (*R*,*S*)-**5**, while the other active

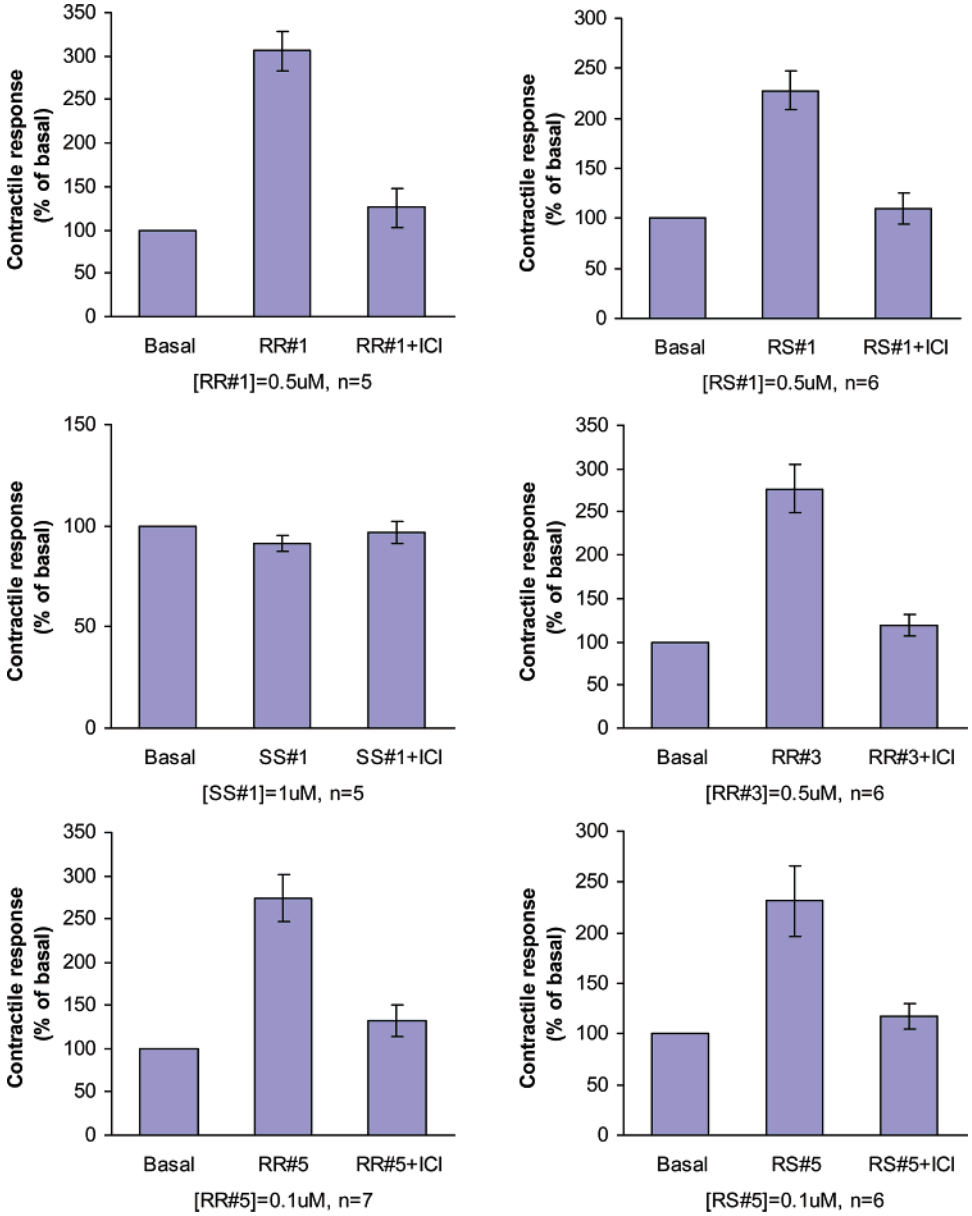

Figure 3. The effect of compounds (*R*,*R*)-**1**, (*R*,*S*)-**1**, (*S*,*S*)-**1**, (*R*,*R*)-**3**, (*R*,*R*)-**5**, and (*R*,*S*)-**5** on cell contraction in single ventricular myocytes isolated from 2 to 4 month old rat hearts after electrical stimulation at 0.5 Hz at 23 °C. Cell length was monitored by an optical edge-tracking method using a photodiode array with a 3 ms time resolution. The experiments were conducted with and without the addition of the selective β_2-AR antagonist ICI 118 551 (10^{-7} mol/L).

compounds required 0.5 μM concentrations. In addition, while the equivalent activities of (*R*,*R*)-**5** and (*R*,*S*)-**5** were suggested by the binding data, the observed activity of (*R*,*S*)-**1** was unexpected, as previous studies of the stereoisomers of **47**[7] and **48**[10] indicated that the agonist activities of the (*R*,*R*)-isomers were significantly greater than the activities of the corresponding (*R*,*S*)-isomers. The full pharmacological profiles of the compounds synthesized in this study are under investigation and will be reported elsewhere.

3D QSAR Modeling. The compounds used in this study were analyzed using comparative molecular field analysis (CoMFA). This is a 3D QSAR technique applicable to the analysis of the relative activities of stereoisomers and/or enantiomers at a selected target, a task usually not approached using regular 2D QSAR.[16,17] The resulting 3D QSAR model shows good statistical correlation with experimental data, $R^2 = 0.920$ and $F = 60.380$, and good prediction power, as indicated by the cross-validated R^2 value (Q^2) = 0.847 and the standard error of prediction (SEP) = 0.309, Table 2.

Two views of the resulting CoMFA model are presented in Figure 4A,B. For visual clarity, only two compounds, (*R*,*R*)-**2** and (*R*,*R*)-**5**, were included in the figures. The chiral centers are depicted as gray balls. The fields are color coded in the following manner: green represents a region of favorable steric (bulk) interactions, unfavorable steric interactions are denoted by yellow, electrostatic interactions with a positive charge (or H-bond donors) are blue, and electrostatic interactions with a negative charge (or H-bond acceptors) are red.

In the first stage, the model was used to identify the regions responsible for the discrimination between the stereoisomers (Figure 4A). The CoMFA procedure produced several distinct asymmetric regions located in close proximity of each chiral center. The first chiral center (carrying the β-hydroxyl group) is surrounded by an electropositive region (large blue region) behind the molecule, Figure 4A. An electropositive region can be associated with hydrogen bond formation and indicates favorable donor properties or unfavorable acceptor properties of the pseudoreceptor. In this case, the location of the electro-

Table 2. The pK_i Predicted by the CoMFA Model

derivative	pK_i measured	pK_i predicted
(*R*,*R*)-**1**	6.46	5.84
(*R*,*S*)-**1**	5.43	5.48
(*S*,*R*)-**1**	4.99	5.02
(*S*,*S*)-**1**	4.56	4.66
(*R*,*R*)-**2**	6.32	6.17
(*R*,*S*)-**2**	5.71	5.80
(*S*,*R*)-**2**	5.28	5.34
(*S*,*S*)-**2**	4.80	4.99
(*R*,*R*)-**3**	5.53	5.57
(*R*,*S*)-**3**	5.10	5.21
(*S*,*R*)-**3**	4.64	4.75
(*S*,*S*)-**3**	4.54	4.39
(*R*,*R*)-**4**	5.73	5.58
(*R*,*S*)-**4**	5.22	5.25
(*S*,*R*)-**4**	4.51	4.75
(*S*,*S*)-**4**	4.54	4.43
(*R*,*R*)-**5**	6.62	6.72
(*R*,*S*)-**5**	6.47	6.36
(*S*,*R*)-**5**	5.75	5.90
(*S*,*S*)-**5**	5.60	5.54
(*R*,*R*)-**6**	5.03	5.01
(*R*,*S*)-**6**	4.50	4.66
(*S*,*R*)-**6**	4.00	4.19
(*S*,*S*)-**6**	4.25	3.84
(*R*)-**7**	4.98	5.33
(*S*)-**7**	4.69	4.51

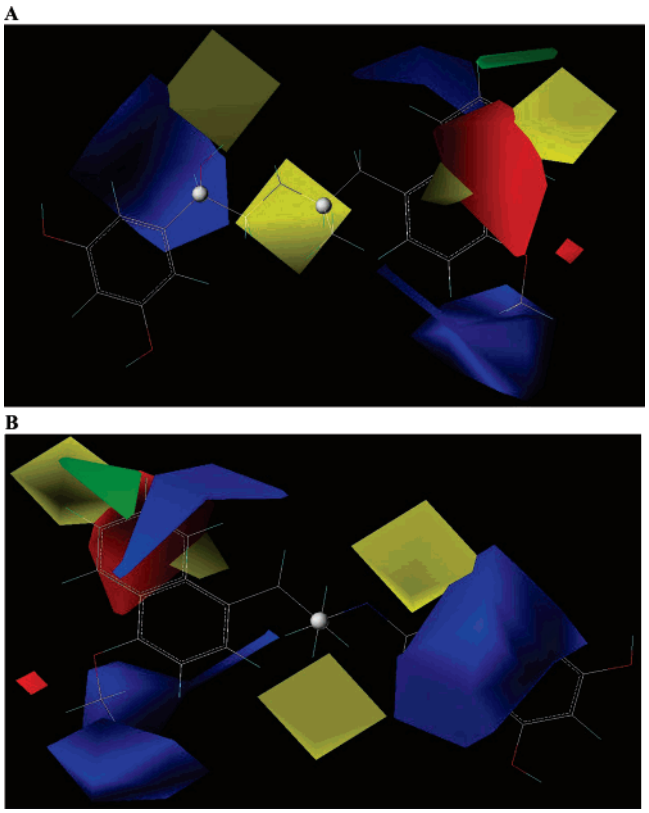

Figure 4. Two views of the resulting CoMFA model. For visual clarity, only two compounds, (*R*,*R*)-**2** and (*R*,*R*)-**5**, were included explicitly in the figures. The chiral centers are depicted as gray balls. The fields are color coded in the following manner: green and yellow represents a region of steric (bulk) interactions (favorable and unfavorable, respectively), electrostatic interactions with a positive charge (or H-bond donor) are blue, and electrostatic interactions with a negative charge (or H-bond acceptor) are red.

positive field indicates that the orientation of the β-OH moiety behind the plane of the model (the *S*-configuration at the chiral center) would hinder H bond formation with the receptor. The electropositive region is closely associated with a steric unfavorable (yellow) region behind the first chiral center. This is an additional indication that the model demonstrates a preference for the β-hydroxyl group in the *R*-configuration. The preference for the *R*-configuration at this center is consistent with previous models and experimental data, which demonstrated that the *R*-configuration is favored for functional activity at β-AR receptors (cf. refs 10−13).

The CoMFA model also demonstrated the effect of the second chiral center. The preferred configuration can be derived from the binding data, where for compounds **1**−**4** and **6** the (*R*,*R*)-isomers had the higher affinities relative to their respective (*R*,*S*)-isomers, while the K_i values for (*R*,*R*)-**5** and (*R*,*S*)-**5** were equivalent, Table 1. Thus, in this model, the more active isomers are those with the methyl moiety on the stereogenic center on the aminoalkyl portion of the molecules pointing out of the plane of the figure of the CoMFA model. This is depicted by a steric disfavoring region (yellow) behind the second chiral center of the molecule and indicates a preference for the *R*-configuration at this site, Figure 4A.

In this study, only the aminoalkyl portion of the fenoterol molecule was altered and, therefore, the key CoMFA regions are associated with this aspect of the molecule. In the resulting analysis, all four interacting regions were identified in the proximity of the aromatic moiety, Figure 4B, and all can be used to generate hypotheses concerning the mode of binding action of the studied derivatives.

In the model, the large electropositive region (blue) encompassing the area close to the −OH or $-OCH_3$ substituents represents H-bond donor properties of the pseudoreceptor to these moieties. These interactions are responsible for the relatively high binding affinities of the O-derivatives, **1** and **2**, relative to **3** and **4**, and in the latter compound, the *p*-amino substituent should be positively charged under the experimental conditions.

A large electronegative region (red) and another electropositive region (blue), both located parallel on two sides of the aromatic system, most likely represent $\pi-\pi$ or π-hydrogen bond interactions between the β_2-AR and electron-rich aromatic moieties, such as the naphthyl ring. This is consistent with the increased affinity of **1**, **2**, and **5** relative to the other compounds examined in this study. The relative importance of this interaction is suggested by the observation that the K_i values for (*R*,*R*)-**5** and (*R*,*S*)-**5** were equivalent to (*R*,*R*)-**1** and (*R*,*R*)-**2**, Table 1.

Two steric regions are located close to the electrostatic regions, and one favors (green) and the other disfavors (yellow) bulkiness in the respective areas. This indicates that the binding of the aminoalkyl portions of the molecules are also sterically restricted.

Discussion

The binding of agonists and antagonists to the β_2-AR has been extensively studied using site-directed mutagenesis and molecular modeling techniques.[11−13,18−20] There is general agreement that the binding of the "catechol" portion of an agonist occurs within a binding area created by the transmembrane (TM) helices identified as TM3, TM5, and TM6. The binding process is a sequential event that produces conformational changes leading to G-protein activation.[19] A key aspect in this process is the interaction of the hydroxyl moiety on the chiral carbon of the agonist with the Asn-293 residue in TM6, and for this interaction, an *R*-configuration is preferable at the chiral carbon.[11,13,20] Because the "catechol" portion of the fenoterol molecule was not altered in this study, it is not surprising that in the CoMFA model, an *R*-configuration at the first stereogenic center is preferred in most stable complexes.

The majority of the binding and functional studies of β_2-AR agonists have been conducted with small *N*-alkyl substituents such as methyl, isopropyl, and *t*-butyl, compare ref 18. However, while these compounds are active at the β_2-AR, they are not subtype selective. This is illustrated by the $K_i\beta_1/K_i\beta_2$ ratios determined for **49**, **50**, and **51** (Figure 2), which were 53, 1.7, and 1.3, respectively.[12] The removal of the *p*-methoxyphenyl moiety not only reduced the selectivity, but also the affinities, as the respective β_2K_i values were 12 nM, 170 nM, and 6300 nM.[12]

The role that aminoalkyl substituents play in β_2-AR selectivity has been investigated using site-directed mutagenesis and molecular modeling techniques.[12,19,20] Using (*R*,*R*)-**49** as the model ligand, Kikkawa et al. determined that hydrogen bond formation between the *p*-methoxy oxygen on **49** and the hydroxyl group of tyrosine 308 (Y308) located in the extracellular end of TM7 was the source of the β_2-AR selectivity.[12]

Furse and Lybrand developed a de novo model of the β_2-AR and investigated molecular complexes of several ligands (agonist and antagonist) with this subtype.[19] Among the structures investigated, (*R*,*R*)-**49** has the same aminoalkyl substituent as the compound **2**. Examination of the (*R*,*R*)-**49**/β_2-AR complex revealed that the *p*-methoxy group oxygen of (*R*,*R*)-**49** formed a hydrogen bond with the hydroxy group of Y308, which supports the model proposed by Kikkawa et al.[12] The distance between the two oxygen atoms bonded in the model was 3.22 Å. However, the methoxy moiety of the ligand was also located in close proximity to three other polar residues, histidine 296 (H296) in TM6, tryptophan 109 (W109) in TM3, and asparagine 312 (N312) in TM7, each of which can interact with an aromatic group on the aminoalkyl portion of (*R*,*R*)-**49**.

In the Furse and Lybrand model, the distance between the oxygen atom of the ligand and the hydrogen atom of H296 was 5.88 Å, and H296 was proposed as an alternative hydrogen bond donor for interaction with the methoxy group of (*R*,*R*)-**49**. Because Y308 and H296 are found only in β_2-AR, with the corresponding residues found in the β_1-AR are F359 and K347, respectively, the interaction with H296 and Y308 has been proposed as the source of β_1/β_2 selectivity.[19]

Because the previous studies of β_1/β_2 selectivity utilized (*R*,*R*)-**49**, the subtype selectivity of the (*R*,*R*)-stereoisomers of the compounds synthesized in our study were compared to the subtype selectivity of (*R*,*R*)-**49**. The data from this study support the hypothesis that hydrogen bond formation between Y308 and/or H296 and the oxygen atom on the *p*-substituent of the agonist is involved in β_2-AR selectivity. The interaction is possible with (*R*,*R*)-**1** and (*R*,*R*)-**2** and the $K_i\beta_1/K_i\beta_2$ ratios for these compounds are 43 and 46, respectively, which are comparable to the $K_i\beta_1/K_i\beta_2$ ratio of 53 determined for (*R*,*R*)-**49**. The $K_i\beta_1/K_i\beta_2$ ratios for **3**, **4**, **6**, and **7** were <10 and reflect the fact that they do not have the ability to form hydrogen bonds with Y308 or H296. The hydrogen bonding interactions were also suggested by the CoMFA model, which identified a large electropositive region (blue) surrounding the area close to the $-$OH or $-OCH_3$ substituents, representing hydrogen-bond donor properties of the pseudoreceptor, Figure 4.

The data from this study also suggest that an aromatic moiety on the aminoalkyl portion of the compound contributes to K_i and subtype selectivity, even if the aromatic moiety is unable to form a hydrogen bond with the receptor. This is demonstrated by the comparison of the $K_i\beta_2$ values for the (*R*,*R*)-isomers of **1**$-$**5**, which were <3.00 μM with $K_i\beta_2$ value of (*R*,*R*)-**6**, which was 9.00 μM, and the $K_i\beta_1/K_i\beta_2$ ratios, which were ≥ 9 for **1**$-$**5**, while **6** displayed no subtype selectivity, Table 1. One possible mechanism to explain the data is π-hydrogen bond formation. The cloud of π-electrons of aromatic rings can act as hydrogen bond acceptors, although it has been estimated that the interaction would be about half as strong as a normal hydrogen bond.[21] The higher affinity and subtype selectivity for (*R*,*R*)-**5** relative to (*R*,*R*)-**3** and (*R*,*R*)-**4** or (*R*)-**7** is consistent with the greater π-electron distribution in the napthyl ring relative to the other aromatic rings.

The CoMFA model also identified a large electronegative region (red) and another electropositive region (blue), both located parallel to the aromatic system, which are most likely associated with $\pi-\pi$ or $\pi-$hydrogen bond interactions between the β_2-AR and electron-rich aromatic moieties, such as the naphthyl ring. Using the model developed by Furse and Lybrand, with (*R*,*R*)-**49** as the interacting ligand, Y308, H296, W109, and N312 were identified as possible sources of $\pi-\pi$ and/or $\pi-$hydrogen bond interactions. In the β_2-AR model, the estimated distances between the *p*-methoxy moiety on (*R*,*R*)-**49** and W109 and N312 were 4.80 Å and 3.45 Å, respectively. Because W109 and N312 are fully conserved in all β-AR subtypes, the interactions suggested by the CoMFA model may represent the source of the increase affinities for (*R*,*R*)-**1**, (*R*,*R*)-**2**, and (*R*,*R*)-**5**, relative to the other (*R*,*R*)-isomers, but not the observed β_1/β_2 selectivity.

The data from this study and the resulting CoMFA model indicate that the binding process of the compounds in this study with the β_2-AR includes the interaction of the chiral center on the aminoalkyl portion of the agonist with a sterically restricted site on the receptor. The existence of a sterically restricted site has been previously suggested from the data obtained in the development of 3D models for agonist and antagonist complexes with the β_2-AR.[18] In these studies, it was observed that for (*R*,*R*)-**49** and similar compounds, substituents larger than a methyl group at the stereogenic center on the aminoalkyl portion would likely produce significant steric interactions that would unfavorably affect the ligand$-$receptor complexes.

The binding of an agonist to the β_2-AR has been described as a multistep interrelated process, in which sequential interactions between the agonist and the receptor produce corresponding conformational changes.[22] The CoMFA model reflects the final agonist/β_2-AR complex, and to discern the effect of the steric restricted site, it is necessary to consider the effect that interaction with this site has on the outcome of the binding process. If one assumes that the interaction of the "catechol" portion of the agonist with the binding area created by TM3, TM5, and TM6 (the first binding area), then these interactions will fix the position of the aminoalkyl portion of the agonist relative to the steric restricted site and perhaps even create this site. In the CoMFA model, the steric restrictions at the site force the methyl moiety at the chiral center of the aminoalkyl portion to point out of the plane of the model, Figure 4A.

It is important to note that due to the free rotation about the N-atom, the configuration at the chiral center bearing the methyl moiety should not affect the ability of the molecule to minimize the interaction with the steric restricted site. However, in the minimum energy conformation, that is, with the methyl group pointing out of the plane of the CoMFA model, the orientation of the remaining segment of the aminoalkyl portion relative to the second binding area would be affected by the stereochemistry. Indeed, *R*- and *S*-configurations would produce mirror image relationships to the second binding area. This situation is illustrated in Figure 5, where the catechol, first chiral center, and the methyl moieties of (*R*,*R*)-**5** and (*R*,*S*)-**5** have been overlaid upon each other.

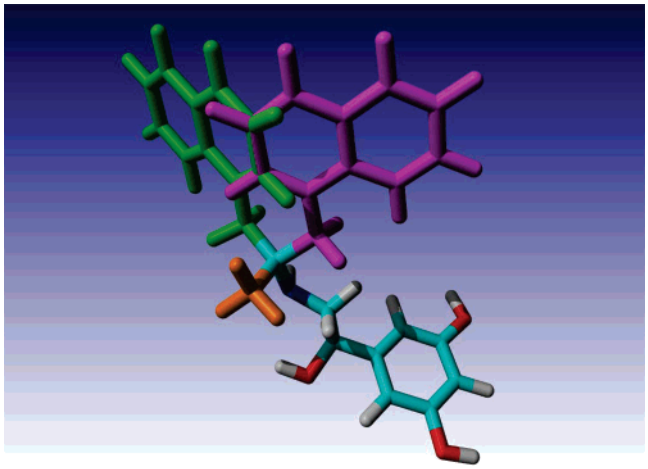

Figure 5. The superimposition of the low-energy conformations for two stereoisomers, (*R*,*R*)-**5** and (*R*,*S*)-**5**. The methyl moiety attached to the second stereogenic center is colored orange, the naphtyl moieties of (*R*,*R*)- and (*R*,*S*)-configurations are green and magenta, respectively; the rest of the molecule is atom type color coded: oxygen, red; nitrogen, blue; carbon, cyan; and hydrogen, white. Note: These conformations are for comparison purpose only and were not intended to recreate the binding conformations within the binding site of the receptor.

The studies elucidating the source of β_2-AR selectivity have primarily utilized (*R*,*R*)-**49** and one previous study of the effect of chirality on subtype selectivity reported that (*R*,*R*)-**47** had a higher β_2-AR selectivity than (*R*,*S*)-**47**.[7] Thus, the observed equivalent affinities and functional activities of (*R*,*R*)-**5** and (*R*,*S*)-**5** at the β_2-AR and the 3-fold increased β_2-AR selectivity of (*R*,*S*)-**5** was an unexpected result. One possible explanation of these results is that the naphthyl moiety of (*R*,*S*)-**5** does not interact with the site defined by Y308 and H296 and is directed toward and binds to another site on the β_2-AR. This interaction also conveys or participates in subtype selectivity as well as increased binding affinity and agonist activity. Because the previous models of β_2-AR selectivity only employed (*R*,*R*)-isomers, it is possible that this site has been overlooked. This possibility is currently under investigation in our laboratory.

Another explanation of the data is suggested by the "rocking tetrahedron" chiral recognition mechanism proposed by Sokolov and Zefirov.[23] In this approach to molecular chiral recognition, the enantiomeric ligands are secured to a chiral selector by two binding interactions. The interactions must be nonequivalent and directional so that only one orientation is possible. The tethered enantiomers still have conformational mobility, and the remaining moieties on the chiral center will sweep out overlapping but not identical steric volumes. Where and to what extent the chiral selector interacts with these steric volumes determines the enantioselectivity of the process. If the chirality of the chiral selector places the interaction perpendicular to the plane of the ligand, no enantioselectivity is observed. As a deviation from the perpendicular increases, so does the enantioselectivity relative to the *R*- or *S*-configuration.

With (*R*,*R*)-**5** and (*R*,*S*)-**5**, the interactions with the first binding area and the steric restricted site of the CoMFA model are two nonequivalent and directional interactions that place the remaining constituents on the second chiral center in the same, albeit mirror image, orientation relative to the second binding area, Figure 5. As discussed above, it is reasonable to assume that the interactions of the 1-naphthyl moieties of **5** with Y308 and H296 are the source of the observed β_2-AR selectivity. If we assume that the 1-naphthyl rings sweep out overlapping but not identical steric volumes, then the observed $K_i\beta_2$ values and subtype selectivity suggest the following: (1) the $K_i\beta_2$-AR values represent the sum total of the π-hydrogen bond and $\pi-\pi$ interactions between the 1-naphthyl moieties and Y308 and H296, as well as additional non-β_2-AR specific interactions with other residues such as W109 and N312; (2) the steric volume swept out by (*R*,*S*)-**5** increases the probability of interactions of Y308 and H296 with the π cloud of the naphthyl moiety relative to the (*R*,*R*)-**5**; (3) the steric volume swept out by (*R*,*R*)-**5** increases the probability of interactions with non-β_2-AR specific sites relative to (*R*,*S*)-**5**.

The effect of the configuration at the second chiral center and conformational-based chiral selectivity is also illustrated by the affinities and subtype selectivities of (*R*,*R*)-**3**, (*R*,*S*)-**3**, and (*R*)-**7**, Table 1. The inversion of the chirality at the second chiral carbon from *R* to *S* reduced the $K_i\beta_2$ value of the (*R*,*S*)-**3**/β_2-AR complex relative to the (*R*,*R*)-**3**/β_2-AR complex by ~3-fold, while there was no significant difference between their $K_i\beta_1$ values. The increased subtype selectivity observed for (*R*,*R*)-**3** relative to (*R*,*S*)-**3**, 9 versus 4, respectively, essentially reflects the differences in $K_i\beta_2$ values, which could be a reflection of increased conformational energy required to bring the aromatic portion of the aminoalkyl chain into contact with the electropositive and electronegative regions that comprise the second binding area or a decrease in the probability that this interaction would occur.

The removal of the methyl moiety on the second chiral center, and thereby the chirality at this site, that is, (*R*)-**7**, had essentially the same effect as inverting the chirality at this site from *R* to *S*. The $K_i\beta_2$ values for (*R*)-**7** was 32% higher than (*R*,*S*)-**3**, and there was no difference in the β_2-AR selectivity, Table 1. These results suggest that for compound **3** the primary effect of the *R*-configuration at the second chiral site was to direct the aminoalkyl chain toward the second binding area, which increased the probability of interacting with this site and reduced the conformational energy required to achieve this interaction.

The primary difference between compounds **3** and **5** is the steric areas swept out by the aromatic substituents. In the case of **3**, the phenyl ring produces a smaller, more linear area, while with **5**, the 1-naphthyl ring system produces a relatively larger and broader area. These differences will be used to guide the synthesis of additional derivatives, which will be used in a more extensive study of the binding of these derivatives to molecular models of the β_2-AR and β_1-AR. The results of these studies will be reported elsewhere.

Based upon the results of this study, (*R*,*R*)-**2** and (*R*,*S*)-**5** have been chosen as possible candidates for the development of a new selective β_2-AR agonist. These compounds may have increased and extended systemic exposures relative to the commercially available *rac*-**1** due to changes in molecular hydrophobicity, metabolic profile, and transporter interactions. The pharmacological and clinical properties of these compounds are under investigation, and the results will be reported elsewhere.

Experimental Section

Membrane Binding Studies. General Procedures. Compounds were tested up to three times each to determine their binding affinities at the β_1- and β_2-adrenergic receptors. Competition curves with standard and unknown compounds included at least six concentrations (in triplicate). For each compound, graphs were prepared containing individual competition curves obtained for that test compound. IC_{50} values and Hill coefficients were calculated using Prism software. K_i values were calculated using the Cheng–Prusoff transformation.[9] In each experiment, a standard compound was simultaneously run on the 96-well plate. If the standard

compound did not have an IC_{50} value close to the established average for that compound, the entire experiment was discarded and repeated again.

β_1-Adrenergic Receptors. β_1-Adrenergic receptor binding was done on rat cortical membrane following a previously described procedure.[15] In brief, male Sprague−Dawley rats weighing 250−350 g were decapitated, and their brains were quickly removed. The cerebral cortices were dissected on ice, weighed, and promptly transferred to a 50 mL test tube containing approximately 30 mL of 50 mM Tris-HCl, pH 7.8 (at room temperature). The tissues were homogenized with a polytron and centrifuged at 20 000 × *g* for 12 min at 4 °C. The pellet was washed again in the same manner and resuspended at a concentration of 20 mg (original wet wt) per 1 mL in the assay buffer (i.e., 20 mM Tris-HCl, 10 mM $MgCl_2$, 1 mM EDTA, 0.1 mM ascorbic acid at pH 7.8). To block the β_2 sites present in the cortical membrane preparation, 30 nM ICI 118-551 was also added to the assay buffer. To wells containing 100 μL of the test drug and 100 μL of [^{3}H]CGP-12177 (1.4 nM final concn), 0.8 mL of tissue homogenate was added. After 2 h at 25 °C, the incubation was terminated by rapid filtration. Nonspecific binding was determined by 10 μM propranolol.

β_2-Adrenergic Receptors. HEK 293 cells stably transfected with cDNA encoding human β_2-AR (provided by Dr. Brian Kobilka, Stanford Medical Center, Palo Alto, CA) were grown in Dulbecco's modified Eagle medium (DMEM) containing 10% fetal bovine serum (FBS), 0.05% penicillin-streptomycin, and 400 μg/mL G418 as previously described.[8] The cells were scraped from the 150 × 25 mm plates and centrifuged at 500 × *g* for 5 min. The pellet was homogenized in 50 mM Tris-HCl, pH 7.7, with a Polytron, centrifuged at 27 000 × *g*, and resuspended in the same buffer. The latter process was repeated, and the pellet was resuspended in 25 mM Tris-HCl containing 120 mM NaCl, 5.4 mM KCl, 1.8 mM $CaCl_2$, 0.8 mM $MgCl_2$, and 5 mM glucose, pH 7.4. The binding assays contained 0.3 nM [^{3}H]CGP-12177 in a volume of 1.0 mL. Nonspecific binding was determined by 1 μM propranolol.

Cardiomyocyte Contractility. These experiments were carried out using a previously described approach.[6] In brief, single ventricular myocytes were isolated from 2 to 4 month old rat hearts by a standard enzymatic technique. The isolated cells were resuspended in HEPES buffer solution [20 mM, pH 7.4] containing NaCl (137 mM), KCl (5.4 mM), $MgCl_2$ (1.2 mM), NaH_2PO_4 (1.0 mM), $CaCl_2$ (1.0 mM), and glucose (20 mM). All experiments were performed within 8 h of cell isolation.

The cells were placed on the stage of an inverted microscope (Zeiss model IM-35, Zeiss, Thornwood, NY), perfused with the HEPES-buffered solution at a flow rate of 1.8 mL/min and electrically stimulated at 0.5 Hz at 23 °C. Cell length was monitored by an optical edge-tracking method using a photodiode array (model 1024 SAQ, Reticon, Boston, MA) with a 3 ms time resolution. Cell contraction was measured by the percent shortening of cell length following electrical stimulation.

Comparative Molecular Field Analysis (CoMFA). In the present work, CoMFA was performed as implemented in Sybyl 7.2. (TRIPOS Inc., St. Louis, MO). Molecular models of all derivatives were prepared in HyperChem v. 6.03 (HyperCube Inc., Gainesville, FL) using ModelBuild procedure to ensure the same conformation of the scaffold. Then the models were extracted to Sybyl, and the partial atomic charges (Gasteiger−Huckel type) were calculated. The models of ligands were aligned using as a common substructure of the two asymmetric carbon atoms in the core of the fenoterol molecule (−C*−CH_2−NH−C*−CH_2−). Next, two types of molecular fields (steric and electrostatic) were sampled on the grid (2 Å spacing) lattice surrounding each structure. Distance-dependent dielectric constant was used in electrostatic calculations and energetic cutoffs of 30 kcal/mol for both the steric and the electrostatic energies were set.

The partial least-square correlation procedure applied for resultant database extracted four statistically significant components, and the following validation parameters were obtained for the best solution: $R^2 = 0.920$, $F(4,21) = 60.380$, standard error of estimate = 0.223, and cross-validated (leave-one-out) $R^2 = 0.847$. In general, electrostatic fields account for 48.1% of explained variance, and steric fields account for 51.9%.

Chemistry. All reactions were carried out using commercial grade reagents and solvents. THF was dried by refluxing over sodium and benzophenone. Dichloromethane was dried by refluxing over calcium hydride. Ultraviolet spectra were recorded on a Cary 50 Concentration spectrophotometer. Optical rotations were done on a Rudolph Research Autopol IV. NMR Spectra were recorded on a Varian Mercury VMX 300-MHz spectrophotometer using tetramethylsilane as the internal standard. In reporting the NMR multiplicities, we used the following abbreviations: s, singlet; d, doublet; t, triplet; q, quartet; p, pentet; m, multiplet; and br, broad. Low-resolution mass spectra were obtained on a Finnigan LCQ^{Duo} LC MS/MS atmospheric pressure chemical ionization (API) quadrupole ion trap MS system equipped with both electrospray (ESI) and atmospheric pressure chemical ionization (APCI) probes. Analytical HPLC data was obtained using a Waters 2690 Separations Module with PDA detection. Method (a): ThermoHypersil BDS 100 × 4.6 mm C18 column, H_2O/CH_3CN/TFA. Method (b): Brownlee Phenyl Spheri-5 100 × 4.6 mm, water/acetonitrile/TFA. Method (c): Vydac 150 × 4 mm C18 column, H_2O /isopropanol/TFA. Method (d): Chiralpak AD-H 250 × 10 mm, 95/5/0.05 CH_3-CN /isopropanol/diethylamine. Merck silica gel (230−400 mesh) was used for open column chromatography.

3′,5′-Dibenzyloxy-α-bromoacetophenone (46). A solution of 2.4 mL (46 mmol) of Br_2 in 45 mL of $CHCl_3$ was added dropwise over 1 h to a chilled, stirring solution of 9.66 g (29 mmol) of 3′,5′-dibenzyloxyacetophenone **45** in 40 mL of $CHCl_3$. The resulting solution was allowed to warm to rt over 1 h with good stirring, then poured into 100 mL of cold H_2O and transferred to a separatory funnel, where the $CHCl_3$ fraction was isolated, washed with brine solution, dried (Na_2SO_4), filtered, and concentrated to 10.8 g. This material was applied to 500 g of silica gel, eluting with $CHCl_3$ to obtain 2.65 g (22%) of **46** as a white solid. ^{1}H NMR ($CDCl_3$) δ 4.39 (s, 2H), 5.08 (s, 4H), 6.85 (t, 1H, $J = 2.1$ Hz), 7.20 (d, 2H, $J = 2.4$ Hz), 7.31−7.44 (m, 10H).

General Procedure for the Enantioselective Reduction of 46 to 3′,5′-Dibenzyloxyphenylbromohydrins [(*R*)-8, (*S*)-8]. Under an argon atmosphere, ∼0.06 mL (0.316 mmol, 10 mol %) of 5.0 M boron−methyl sulfide complex (BH_3SCH_3)in diethyl ether was added in one portion to a solution of 25 mg (0.16 mmol, 5 mol %) of the appropriate *cis*-1-amino-2-indanol in 3 mL of dry THF. This material under argon was added over 30 min to a solution of 1.3 g (3.16 mmol) of 3′,5′-dibenzyloxy-α-bromoacetophenone **46** in 20 mL of dry THF, while at the same time adding in ∼0.05 mL pulses 0.45 mL of 5.0 M boron−methyl sulfide complex. The resulting solution was allowed to stir under argon for 2 h and then quenched with 3 mL of methanol, controlling gas evolution. Solvents were removed in vacuo, and the resulting residue was taken up in 30 mL of $CHCl_3$ and washed with 25 mL of 0.2 M sulfuric acid followed by 20 mL of brine and then dried (Na_2SO_4), filtered, and evaporated.

(*R*)-(−)-3′,5′-Dibenzyloxyphenylbromohydrin [(*R*)-8]. (*R*)-**8** was prepared with (1*R*,2*S*)-(+)-*cis*-1-amino-2-indanol as the enantioselective reduction catalyst to give 1.02 g (78%) of (*R*)-**8** as a fine white powder. ^{1}H NMR ($CDCl_3$) δ 3.44 (dd, 1H, $J = 9.0$, 10.5 Hz), 3.55 (dd, 1H, $J = 3.3$, 10.5 Hz), 4.79 (dd, 1H, $J = 3.3$, 8.7 Hz), 4.97 (s, 4H), 6.51 (t, 1H, $J = 2.4$ Hz), 6.57 (d, 2H, $J = 1.8$ Hz), 7.21−7.38 (m, 10H); $[\alpha]_D = -12.1°$ (*c* 1.0, MeOH).

(*S*)-(+)-3′,5′-Dibenzyloxyphenylbromohydrin [(*S*)-8]. (*S*)-**8** was prepared with (1*S*,2*R*)-(-)-*cis*-1-amino-2-indanol as the enantioselective reduction catalyst to give 1.07 g (82%) of (*S*)-**8** as a fine white powder. ^{1}H NMR ($CDCl_3$) δ 3.43 (dd, 1H, $J = 9.0$, 10.5 Hz), 3.55 (dd, 1H, $J = 3.3$, 10.5 Hz), 4.78 (dd, 1H, $J = 3.3$, 8.7 Hz), 4.96 (s, 4H), 6.50 (t, 1H, $J = 2.4$ Hz), 6.57 (d, 2H, $J = 1.8$ Hz), 7.21−7.39 (m, 10H); $[\alpha]_D = +11.8°$ (*c* 0.90, MeOH).

4-Benzyloxyphenylacetone (34). To 10.0 g (41.3 mmol) of 4-benzyloxyphenylacetic acid **31** (Aldrich) was added 20 mL of acetic anhydride and 20 mL of pyridine, which was heated to reflux with stirring under an argon atm for 6 h. Solvents were evaporated, and the residue was dissolved in $CHCl_3$ (50 mL) and washed with

1 N NaOH (2 × 50 mL). The organic layer was dried ($MgSO_4$), filtered, and evaporated to 11.8 g of an amber oil. Vacuum distillation at 0.1 mmHg in an oil bath set to 170 °C, followed by silica gel chromatography eluting with 8/2 CH_2Cl_2−hexanes, gave 2.68 g (27%). ^{1}H NMR ($CDCl_3$) δ 2.14 (s, 3H), 3.63 (s, 2H), 5.05 (s, 2H), 6.94 (d, 2H, J = 8.7 Hz), 7.10 (d, 2H, J = 8.7 Hz), 7.26−7.47 (m, 5H).

Phenylacetone (35). A solution of 20.4 g (0.15 mol) of phenylacetic acid **32** (Aldrich), acetic anhydride (70 mL), and pyridine (70 mL) was heated to reflux with stirring under an argon atm for 6 h. Solvents were evaporated, the residue was dissolved in $CHCl_3$ (100 mL) and washed with 1 N NaOH (2 × 100 mL), and the organic layer was dried ($MgSO_4$), filtered, and evaporated to give 20.4 g. Vacuum distillation at 0.1 mmHg in an oil bath set to 160 °C, followed by silica gel chromatography eluting with 1/1 hexanes/CH_2Cl_2, gave 5.5 g (27%). ^{1}H ($CDCl_3$) δ 2.15 (s, 3H), 3.70 (s, 2H), 7.20−7.36 (m, 5H).

1-Naphthalen-1-yl-propan-2-one (36). A solution of 37.2 g (20 mmol) of naphthoic acid **33** (Aldrich), acetic anhydride (100 mL), and pyridine (100 mL) was heated to reflux with stirring under an argon atm for 6 h. The solvents were evaporated, the residue was dissolved in $CHCl_3$ (200 mL) and washed with 1 N NaOH (2 × 150 mL), and the organic layer was dried ($MgSO_4$), filtered, and evaporated to give 34.6 g. Distillation at 0.5 mmHg in an oil bath set to 170 °C, followed silica gel chromatography eluting with 1/1 hexanes/CH_2Cl_2, gave 9.7 g (26%). ^{1}H ($CDCl_3$) δ 2.11 (s, 3H), 4.12 (s, 2H), 7.40−7.53 (m, 4H), 7.81 (d, 1H, J = 8.4 Hz), 7.87−7.90 (m, 2H).

General Procedure for Preparation of 2-Benzylaminopropanes (37−39, 42, 43). To the appropriate ketone (1 equiv) in CH_2Cl_2 (c = 0.5 M), cooled to 0 °C, was added glacial HOAc (1 equiv), followed by benzylamine (1 equiv) and $NaBH(AcO)_3$ (1.4 equiv), and the mixture was then warmed to rt and stirred under argon for 20 h. The reaction mixture was cooled (ice bath), and 10% NaOH (5 equiv) was added dropwise and then extracted into CH_2Cl_2, washed with brine, dried (Na_2SO_4), filtered, and evaporated.

1-(4-Benzyloxy)-2-benzylaminopropane (37). Compound **37** was prepared from 4-benzyloxy-phenylacetone **34** (2.0 g, 8.3 mmol) to afford 2.61 g (95%) as a tan solid. ^{1}H ($CDCl_3$) δ 1.10 (d, 3H, J = 6.3 Hz), 2.50−2.58 (m, 1H), 2.68−2.77 (m, 1H), 2.82−2.89 (m, 1H), 3.75 (dd, 2H, J = 12 Hz, J = 30 Hz), 5.05 (s, 2H), 6.90 (d, 2H, J = 8.7 Hz), 7.04 (d, 2H, J = 8.7 Hz), 7.17−7.42 (m, 10H); MS (APCI+) m/z (rel) 332 (100).

1-Phenyl-2-benzylaminopropane (38). Compound **38** was prepared from phenylacetone **35** (5.5 g, 41 mmol) to afford 8.4 g (91%) as a tan solid. ^{1}H ($CDCl_3$) δ 1.09 (d, 3H, J = 6.3 Hz), 2.61−2.81 (m, 2H), 2.92 (m, 1H), 3.80 (dd, 2H), 7.14−7.30 (m, 10H); MS (APCI+) m/z (rel) 226 (100).

1-(1′-Naphthyl)-2-benzylaminopropane (39). Compound **39** was prepared from 1-naphthalen-1-yl-propan-2-one **36** (5.0 g, 27.1 mmol) to afford 7.0 g (94%) as a tan solid. ^{1}H ($CDCl_3$) δ 1.14 (d, 3H, J = 6.0 Hz), 3.02−3.18 (m, 2H), 3.27 (m, 1H), 3.80 (dd, 2H, J = 13.2, 43.8 Hz), 7.13−7.23 (m, 5H), 7.31−7.48 (m, 4H), 7.73 (d, 1H, J = 7.8 Hz), 7.83−7.86 (m, 1H), 7.96−7.99 (m, 1H); MS (APCI+) m/z (rel) 276 (100).

1-(4′-Methoxyphenyl)-2-benzylaminopropane (42). Compound **42** was prepared from 4-methoxyphenylacetone (Aldrich) **40** (2.75 g, 13.1 mmol) to afford 2.31 g (97%). ^{1}H ($CDCl_3$) δ 1.10 (d, 3H, J = 6.3 Hz), 2.56−2.75 (m, 2H), 2.90 (m, 1H), 3.79 (s, 1H), 3.79 (m, 2H, J = 13.2 Hz), 6.82 (d, 2H, J = 8.7 Hz), 7.07 (d, 2H, J = 8.7 Hz), 7.18−7.32 (m, 5H); MS (APCI+) m/z (rel) 256 (100).

1-(4′-Nitrophenyl)-2-benzylaminopropane (43). Compound **43** was prepared from 4-nitrophenylacetone (Aldrich) **41** (4.95 g, 28 mmol) to afford 7.32 g (98%) as an amber oil. ^{1}H ($CDCl_3$) δ 1.60 (d, 3H, J = 6.3 Hz), 2.73−2.85 (m, 1H), 3.00−3.12 (m, 2H), 3.86 (dd, 2H, J = 26 Hz, J = 60 Hz), 7.23−7.40 (m, 5H), 7.30 (d, 2H, J = 9.0 Hz), 8.14 (d, 2H, J = 8.7 Hz); MS (APCI+) m/z (rel) 271 (100).

General Procedure for Enantiomeric Separation of 2-Benzylaminopropanes [(*R*)-10−14, (*S*)-10−14]. The appropriate racemic 2-benzylaminopropane (1 equiv) was combined with the appropriate optically active mandelic acid (1 equiv) in methanol (c = 0.5 M) and refluxed until the solution homogenized, then cooled to rt. The crystals were filtered, collected, and recrystallized twice from methanol (c = 0.3 M) to afford the optically active 2-benzylaminopropane·mandelic acid salt. The salts were converted to the free amine for the purpose of collecting NMR and rotation data by partitioning the mandelic acid salt between 10% K_2CO_3 and $CHCl_3$, drying organic extracts (Na_2SO_4), and evaporating.

(*R*)-(−)-1-(4′-Benzyloxy)-2-benzylaminopropane [(*R*)-10]. A sample of 2.13 g (6.42 mmol) of 1-(4-benzyloxy)-2-benzylaminopropane **37** was reacted with 972 mg (6.42 mmol) of (*R*)-(−)-mandelic acid to give 295 mg (28% based on enantiomeric abundance) of the free amine after workup. ^{1}H NMR ($CDCl_3$) δ 1.12 (d, 3H, J = 6.3 Hz), 2.58−2.78 (m, 2H), 2.82−2.91 (m, 1H), 3.75 (dd, 2H, J = 12 Hz, J = 30 Hz)), 5.07 (s, 2H), 6.93 (d, 2H, J = 8.7 Hz), 7.10 (d, 2H, J = 8.7 Hz), 7.21−7.42 (m, 10H); MS (APCI+) m/z (rel) 332 (100); $[\alpha]_D$ = −19.1° (c 1.4, MeOH).

(*S*)-(+)-1-(4′-Benzyloxy)-2-benzylaminopropane [(*S*)-10]. The washes from the separation of (*R*)-**10** were concentrated and partitioned between 50 mL of chloroform and 50 mL of 10% K_2CO_3 in water. The organics were washed with brine, dried (Na_2SO_4), filtered, and evaporated to give 1.70 g (5.1 mmol), which was brought to reflux with 782 mg (5.1 mmol) of (*S*)-(+)-mandelic acid, as previously described and crystallized three times to obtain 670 mg of the (*S*)-amine·(*S*)-mandelic acid salt. This compound was triturated in ether then partitioned between 30 mL of chloroform and 20 mL of 10% K_2CO_3 in water. The organic partition was washed with brine, dried (Na_2SO_4), filtered, and evaporated to give 366 mg of the free amine (33% based on enantiomeric abundance). ^{1}H NMR ($CDCl_3$) δ 1.10 (d, 3H, J = 6.3 Hz), 2.58−2.78 (m, 2H), 2.82−2.91 (m, 1H), 3.76 (dd, 2H, J = 12, 30 Hz), 5.06 (s, 2H), 6.93 (d, 2H, J = 8.7 Hz), 7.09 (d, 2H, J = 8.7 Hz), 7.21−7.42 (m, 10H); MS (APCI+) m/z (rel) 332 (100); $[\alpha]_D$ = +19.2° (c 1.5, MeOH).

(*R*)-(−)-1-(4′-Methoxyphenyl)-2-benzylaminopropane [(*R*)-11]. A sample of 3.02 g (11.8 mmol) of 1-(4′-methoxyphenyl)-2-benzylaminopropane **42** was reacted with 1.8 g (11.8 mmol) of (*S*)-(+)-mandelic acid to give 530 mg (35% based on enantiomeric abundance) of the free amine after workup. ^{1}H NMR ($CDCl_3$) δ 1.10 (d, 3H, J = 6.3 Hz), 2.57−2.76 (m, 2H), 2.88−2.94 (m, 1H), 3.79 (s, 3H), 3.72−3.88 (m, 2H), 6.82 (d, 2H, J = 8.7 Hz), 7.07 (d, 2H, J = 8.4 Hz), 7.15−7.31 (m, 5H); MS (APCI+) m/z (rel) 256 (100); $[\alpha]_D$ = −30.4° (c 1.25, MeOH).

(*S*)-(+)-1-(4′-Methoxyphenyl)-2-benzylaminopropane [(*S*)-11]. A sample of 3.36 (13.2 mmol) of the racemate 1-(4′-methoxyphenyl)-2-benzylaminopropane **42** was reacted with 2.0 g (13.2 mmol) of (*R*)-(−)-mandelic acid to give 740 mg (44% based on enantiomeric abundance) of the free amine after workup. ^{1}H NMR, ($CDCl_3$) δ 1.10 (d, 3H, J = 6.2 Hz), 2.55−2.76 (m, 2H), 2.88−2.95 (m, 1H), 3.73−3.88 (m, 2H), 3.79 (s, 3H), 6.80 (d, 2H, J = 8.7 Hz), 7.08 (d, 2H, J = 8.4 Hz), 7.15−7.30 (m, 5H); MS (APCI+) m/z (rel) 256 (100); $[\alpha]_D$ = +30.5° (c 1.1, MeOH).

(*R*)-(−)-1-(4′-Nitrophenyl)-2-benzylaminopropane [(*R*)-12]. A sample of 2.0 g (7.3 mmol) of 1-(4′-nitrophenyl)-2-benzylaminopropane **43** was reacted with 1.13 g (7.3 mmol) of (*S*)-(+)-mandelic acid to give 486 mg (49% based on enantiomeric abundance) of the free amine after workup. ^{1}H NMR ($CDCl_3$) δ 1.60 (d, 3H, J = 6.3 Hz), 2.73−2.85 (m, 1H), 3.00−3.12 (m, 2H), 3.86 (dd, 2H, J = 26 Hz, J = 60 Hz), 7.23−7.40 (m, 5H), 7.30 (d, 2H, J = 9.0 Hz), 8.14 (d, 2H, J = 8.7 Hz); MS (APCI+) m/z (rel) 271 (100); $[\alpha]_D$ = −9.3° (c 1.0, MeOH).

(*S*)-(+)-1-(4′-Nitrophenyl)-2-benzylaminopropane [(*S*)-12]. A sample of 2.0 g (7.3 mmol) of 1-(4′-nitrophenyl)-2-benzylaminopropane **43** was reacted with 1.13 g (7.3 mmol) of (*R*)-(−)-mandelic acid to give 640 mg (65% based on enantiomeric abundance) of the free amine after workup. ^{1}H NMR ($CDCl_3$) δ 1.60 (d, 3H, J = 6.3 Hz), 2.73−2.85 (m, 1H), 3.00−3.12 (m, 2H), 3.86 (dd, 2H, J = 26, 60 Hz), 7.23−7.40 (m, 5H), 7.30 (d, 2H, J = 9.0 Hz), 8.14 (d, 2H, J = 8.7 Hz); MS (APCI+) m/z (rel) 271 (100); $[\alpha]_D$ = +8.2° (c 1.0, MeOH).

(*R*)-(−)-1-Phenyl-2-benzylaminopropane [(*R*)-13]. A sample of 2.62 g (11.6 mmol) of 1-phenyl-2-benzylaminopropane **38** was reacted with 1.77 g (11.6 mmol) of (*S*)-(+)-mandelic acid to give 747 mg (57% based on enantiomeric abundance) of the free amine after workup. ^{1}H NMR ($CDCl_3$) δ 1.13 (d, 3H, J = 6.0 Hz), 2.62−2.84 (m, 2H), 2.92−2.99 (m, 1H), 3.81 (dd, 2H, J = 13.2, 34.5 Hz) 7.14−7.29 (m, 10H); MS (APCI+) *m*/*z* (rel) 226 (100); $[\alpha]_D$ = −24.5° (*c* 1.10, MeOH).

(*S*)-(+)-1-Phenyl-2-benzylaminopropane [(*S*)-13]. A sample of 5.0 g (22.2 mmol) of racemic 1-phenyl-2-benzylaminopropane **38** was reacted with 3.4 g (22.2 mmol) of (*R*)-(−)-mandelic acid to give 2.15 g (86% based on enantiomeric abundance) of the free amine after workup. ^{1}H NMR ($CDCl_3$) δ 1.11 (d, 3H, J = 6.0 Hz), 2.62−2.84 (m, 2H), 2.92−2.99 (m, 1H), 3.81 (dd, 2H, J = 13.2, 34.5 Hz), 7.14−7.29 (m, 5H); MS (APCI+) *m*/*z* (rel) 226 (100); $[\alpha]_D$ = +18.2° (*c* 0.85, MeOH).

(*R*)-(−)-1-(1′-Naphthyl)-2-benzylaminopropane [(*R*)-14]. The washes recovered from the separation of [(*S*)-**14**] were concentrated and partitioned between 40 mL of choroform and 40 mL of 10% K_2CO_3 in water. The organic partition was washed with 20 mL of brine then dried (Na_2SO_4) to afford 1.16 g (4.2 mmol) of the free amine, which was reacted with 640 mg (4.2 mmol) of (*S*)-(+)-mandelic acid. A total of 588 mg (46% based on enantiomeric abundance) of the free amine was obtained. ^{1}H NMR ($CDCl_3$) δ 1.07 (d, 3H, J = 6.0 Hz), 3.02−3.18 (m, 2H), 3.27 (m, 1H), 3.74 (dd, 2H, J = 13.2, 30.9 Hz), 7.13−7.23 (m, 5H), 7.31−7.48 (m, 4H), 7.73 (d, 1H, J = 7.8 Hz), 7.83−7.86 (m, 1H), 7.96−7.99 (m, 1H); MS (APCI+) *m*/*z* (rel) 276 (100); $[\alpha]_D$ = −5.8° (*c* 1.0, MeOH).

(*S*)-(+)-1-(1′-Naphthyl)-2-benzylaminopropane [(*S*)-14]. A sample of 2.6 g (9.4 mmol) of 1-(1′-naphthyl)-2-benzylaminopropane, **39**, was reacted with 1.44 g (9.4 mmol) of (*R*)-(−)-mandelic acid to give 420 mg (21% based on enantiomeric abundance) of the free amine after workup. ^{1}H NMR ($CDCl_3$) δ 1.07 (d, 3H, J = 6.0 Hz), 3.02−3.18 (m, 2H), 3.27 (m, 1H), 3.74 (dd, 2H, J = 13.2, 30.9 Hz), 7.13−7.23 (m, 5H), 7.31−7.48 (m, 4H), 7.73 (d, 1H, J = 7.8 Hz), 7.83−7.86 (m, 1H), 7.96−7.99 (m, 1H); MS (APCI+) *m*/*z* (rel) 276 (100); $[\alpha]_D$ = +6.3° (*c* 1.0, MeOH).

(*R*)-(−)-2-Benzylaminoheptane [(*R*)-15]. A sample of 0.65 mL (4.4 mmol) of (*R*)-(−)-2-aminoheptane, *R*-**44**, 0.44 mL (4.4 mmol) of benzaldehyde, and 0.1 mL of HOAc were combined in 40 mL of CH_2Cl_2 and then cooled to 0 °C. To the reaction mixture was added 2.75 mg (13 mmol) of sodium triacetoxyborohydride in one portion, which was stirred under argon at rt for 28 h, diluted with 30 mL of CH_2Cl_2, and cooled in ice bath. An aliquot of 80 mL of 5% NaOH in water was added, fractions were separated, and the organics were dried (Na_2SO_4) and evaporated to 638 mg (71%) of **(*R*)-15**. ^{1}H NMR ($CDCl_3$) δ 0.88 (m, 3H), 1.08 (d, 3H J = 6.6 Hz), 1.20−1.39 (m, 6H), 1.41−1.67 (m, 2H), 3.62−3.77 (m, 1H), 3.75 (p, 2H, J = 12 Hz), 7.17−7.41 (m, 5H); MS (APCI+) *m*/*z* (rel) 206 (100); $[\alpha]_D$ = +6.9° (*c* 1.0, MeOH).

(*S*)-(+)-2-Benzylaminoheptane [(*S*)-15]. A sample of 0.15 mL (1 mmol) of (*S*)-(+)-2-aminoheptane, (*S*)-**44**, 0.1 mL (1 mmol) of benzaldehyde, and 0.1 mL of HOAc were combined in 10 mL of CH_2Cl_2 and cooled to 0 °C, then 650 mg (3 mmol) of sodium triacetoxyborohydride was added in one portion. The reaction mixture was stirred under argon at rt for 28 h, the mixture was diluted with 10 mL of dichloromethane and cooled in ice bath, and 20 mL of 5% NaOH in water was added. Fractions were separated, and the organics were dried (Na_2SO_4) and evaporated to 154 mg (70%). ^{1}H NMR ($CDCl_3$) δ 0.88 (m, 3H), 1.08 (d, 3H J = 6.6 Hz), 1.19−1.37 (m, 6H), 1.41−1.67 (m, 2H), 3.62−3.77 (m, 1H), 3.75 (p, 2H, J = 12 Hz), 7.17−7.41 (m, 5H); MS (APCI+) *m*/*z* (rel) 206 (100); $[\alpha]_D$ = +7.8° (*c* 1.0, MeOH).

Preparation of Fenoterol Analogs, Procedure A. To form the epoxide, the appropriate 3′,5′-dibenzyloxyphenylbromohydrin (*R*)-**8** or (*S*)-**8** (1 equiv) was combined with K_2CO_3 (1.4 equiv) in 1:1 THF/MeOH (c = 0.3 M) and stirred for 2 h under argon at rt. The solvent was removed, and the residue was partitioned between toluene and H_2O. The toluene fraction was isolated and dried (Na_2SO_4), filtered, and evaporated. The residue was dissolved with the appropriate free benzylamine (*R*)- or (*S*)-**10**−**15**, **28** (0.95 equiv) in a good amount of toluene and evaporated again under high vacuum to remove trace H_2O. The resulting colorless residue was heated to 120 °C under argon for 20 h, cooled, and checked by ^{1}H NMR and mass spectrometry to confirm coupling. The residue was dissolved in EtOH (c = 0.07 M) with heat and transferred to a Parr flask, where it was hydrogenated at 50 psi of hydrogen over 10% (wt) Pd/C (10 mg cat/65 mg bromohydrin) for 24 h. Complete debenzylation was confirmed by mass spectrometry. The mixture was filtered through Celite, the filter cake was rinsed with isopropanol, and the filtrate was concentrated. The residue was dissolved in 1:1 isopropanol/EtOH (c = 0.2 M) and brought to reflux for 30 min with 0.5 equiv of fumaric acid. The reaction was cooled and the solvent was removed. The crude material was purified by open column chromatography or preparative chromatography.

Column Separation of (*R*,*R*)-1 and (*S*,*S*)-1, Procedure B. A sample of 75 mg of fenoterol HBr (Aldrich) was dissolved in 1.5 mL of 95/5/0.05 CH_3CN/isopropanol/$HNEt_2$ and applied in 100 μL injections to a Chiralpak AD-H 10 × 250 mm 5 μm semipreparative column using a Waters 2690 Separations Module, with PDA set to 280 nm. The eluting solvent was 95/5/0.05 CH_3CN/isopropanol/$HNEt_2$, 5 mL/min. Retention times for (*S*,*S*)- and (*R*,*R*)-isomers were 4.8 and 7.8 min, respectively.

(*R*,*R*)-(−)-Fenoterol [(*R*,*R*)-1]. *R*,*R*-**1** was obtained according to procedure B to give 40 mg, which was collected after evaporation. ^{1}H NMR (CD_3OD) δ 1.05 (d, 3H, J = 6.3 Hz), 2.49 (q, 1H, J = 6.9 Hz), 2.62−2.74 (m, 2H), 2.80−2.91 (m, 2H), 4.55 (dd, 1H, J = 5.1, J = 3.3 Hz), 6.16 (t, 1H, J = 2.4 Hz), 6.27 (d, 2H, J = 2.1 Hz), 6.68 (d, 2H, J = 8.4 Hz), 6.94 (d, 2H, J = 8.4 Hz); ^{13}C NMR (CD_3CN) δ 20.3, 43.2, 55.1, 55.2, 72.4, 102.2, 105.4, 116.0, 131.3, 131.8, 147.4, 156.2, 159.0; UV (MeOH) λ_{max} 279 nm (ϵ 2760), 225 (12 900), 204 (32 600); MS (APCI+) *m*/*z* (rel) 304 (100, M + H); $[\alpha]_D$ = −29.0° (*c* 0.2, MeOH); HPLC (a) 0.1% diethylamine in H_2O, 0.50 mL/min, 254 nm, t_R 2.90 min, 99% pure; (d) t_R 7.8 min, >99% pure.

(*S*,*S*)-(+)-Fenoterol [(*S*,*S*)-1]. *S*,*S*-**1** was obtained according to procedure B to give 35 mg after evaporation. ^{1}H NMR (CD_3OD) δ 1.05 (d, 3H, J = 6.6 Hz), 2.49 (q, 1H, J = 7.2 Hz), 2.62−2.76 (m, 2H), 2.80−2.94 (m, 2H), 4.55 (dd, 1H, J = 4.8, J = 3.3 Hz), 6.16 (t, 1H, J = 2.1 Hz), 6.27 (d, 2H, J = 2.4 Hz), 6.68 (d, 2H, J = 8.4 Hz), 6.94 (d, 2H, J = 8.4 Hz); ^{13}C (CD_3CN) δ 20.3, 43.2, 55.0, 55.2, 72.4, 102.2, 105.4, 116.0, 131.3, 131.8, 147.4, 156.2, 159.0; UV (MeOH) λ_{max} 279 nm (ϵ 2680), 224 (12 700), 204 (32 800); MS (APCI+) *m*/*z* (rel) 304 (100, M + H); $[\alpha]_D$ = +28.5° (*c* 0.20, MeOH); HPLC (a) 0.1% diethylamine in H_2O, 0.50 mL/min, 254 nm, t_R 2.72 min, >99% pure; (d) t_R 4.8 min, >99% pure.

(*R*,*S*)-(−)-Fenoterol Fumarate [(*R*,*S*)-1]. *R*,*S*-**1** was prepared from (*R*)-**8** and (*S*)-**10** according to procedure A to give 168 mg (64%). ^{1}H NMR (CD_3OD) δ 1.22 (d, 3H, J = 6.6 Hz), 2.64 (dd, 1H, J = 9.9 Hz, J = 13.2 Hz), 3.01−3.51 (m, 4H), 4.79 (dd, 1H, J = 3.0 Hz, J = 9.9 Hz), 6.23 (t, 1H, J = 2.4 Hz), 6.36 (d, 2H, J = 2.1 Hz), 6.75 (s, 1H), 6.76 (d, 2H, J = 8.4 Hz), 7.05 (d, 2H, J = 8.1 Hz); ^{13}C NMR (CD_3OD) δ 16.2, 39.1, 52.5, 57.4, 70.4, 103.4, 105.3, 116.7, 127.8, 131.4, 135.2, 144.6, 157.7, 160.0, 168.2; UV (MeOH) λ_{max} 278 nm (ϵ 2520), 205 (27 900); MS (ESI+) *m*/*z* (rel) 304 (100, M + H); $[\alpha]_D$ = −7.5° (*c* 0.75, MeOH); HPLC (a) 70/30/0.05 1.00 mL/min, 282 nm, t_R 1.35 min, >99% pure; (b) 50/50/0.05 1.0 mL, 0.50 mL/min, 254 nm, t_R 2.72 min, >99% pure; (d) t_R 4.8 min, 1.00 mL/min, 280 nm, t_R 2.10 min, 97.5% pure.

(*S*,*R*)-(+)-Fenoterol Fumarate [(*S*,*R*)-1]. *S*,*R*-**1** was prepared from (*S*)-**8** and (*R*)-**10** according to procedure A to give 104 mg (39%). ^{1}H NMR (CD_3OD) δ 1.22 (d, 3H, J = 6.6 Hz), 2.64 (dd, 1H, J = 9.9 Hz, J = 13.5 Hz), 3.47−3.04 (m, 4H), 4.80 (dd, 1H, J = 2.7, J = 9.6 Hz), 6.23 (t, 1H, J = 2.4 Hz), 6.36 (d, 2H, J = 2.1 Hz), 6.75 (s, 1H), 6.76 (d, 2H, J = 8.4 Hz), 7.05 (d, 2H, J = 8.4 Hz); ^{13}C NMR (CD_3OD) δ 16.2, 39.1, 52.5, 57.4, 70.4, 103.4, 105.3, 116.7, 127.8, 131.4, 135.2, 144.6, 157.7, 159.9, 168.2; UV (MeOH) λ_{max} 278 nm (ϵ 2640), 202 (36 600); MS (ESI+) *m*/*z* (rel) 304 (100, M + H), 413 (10); $[\alpha]_D$ = +6.4° (*c* 0.50, MeOH); HPLC

(a) 70/30/0.05, 1.00 mL/min, 282 nm, t_R 1.35 min, 95.9% pure; (b) 50/50/0.05, 1.0 mL/min, 280 nm, t_R 2.06 min, 99% pure.

(*R*,*R*)-(−)-1-*p*-Methoxyphenyl-2-(β-3′,5′-dihydroxyphenyl-β-oxy)ethylamino-propane Fumarate [(*R*,*R*)-2]. *R*,*R*-**2** was prepared from (*R*)-**8** and (*R*)-**11** according to procedure A to give 172 mg (38%). ^{1}H NMR (CD_3OD) δ 1.08 (d, 3H, J = 6.3 Hz), 3.05−2.56 (m, 5H), 4.57 (dd. 1H, J = 8.4, 5.4 Hz), 6.16 (m, 1H), 6.26 (d, 2H, J = 2.7 Hz), 6.81 (d, 2H, J = 8.7 Hz), 7.03 (d, 2H J = 8.7 Hz); ^{13}C NMR (CD_3OD) δ 18.8, 42.3, 54.5, 55.6, 56.0, 72.6, 103.0, 105.4, 115.0, 131.1, 131.2, 131.3, 146.2, 159.8, 159.9; UV (MeOH) λ_{max} 277 nm (ε 3590), 224 (17 700), 207 (29 500); MS (ESI+) *m*/*z* (rel) 318 (100, M + H); $[\alpha]_D$ = −24.9° (*c* 0.8, MeOH); HPLC (a) 70/30/0.05, 1.0 mL/min, 282 nm, t_R 1.54 min, 96.5% pure; (b) 50/50/0.05, 2.0 mL/min, 276 nm, t_R 1.51 min, 95.9% pure.

(*S*,*S*)-(+)-1-*p*-Methoxyphenyl-2-(β-3′,5′-dihydroxyphenyl-β-oxy)ethylamino-propane Fumarate [(*S*,*S*)-2]. *S*,*S*-**2** was prepared from (*S*)-**8** and (*S*)-**11** according to procedure A to give 318 mg (53%). ^{1}H NMR (CD_3OD) δ 1.15 (d, 3H, J = 6.0 Hz), 2.58−3.22 (m, 5H), 3.77 (s, 3H), 4.68 (dd, 1H, J = 4.8, 8.4 Hz), 6.18 (t, 1H, J = 2.1 Hz), 6.31 (d, 2H, J = 2.1 Hz), 2.23 (s, 0.5 H, fumarate), 6.84 (d, 2H, J = 8.7 Hz), 7.10 (d, 2H, J = 9.0 Hz); ^{13}C NMR (CD_3OD) δ 16.1, 39.9, 52.4, 54.5, 55.3, 70.4, 101.9, 104.2, 114.0, 129.2, 130.1, 144.4, 158.7, 158.9; UV (MeOH) λ_{max} 277 nm (ε 2100), 224 (1100), 205 (22 700); MS (ESI+) *m*/*z* (rel) 318 (100, M + H); $[\alpha]_D$ = +28.6° (*c* 0.95, MeOH); HPLC (a) 70/30/0.05, 1.0 mL/min, 282 nm, t_R 1.67 min, 96.0% pure; (b) 50/50/0.05, 2.0 mL/min, 276 nm, t_R 1.51 min, 97.1% pure.

(*R*,*S*)-(−)-1-*p*-Methoxyphenyl-2-(β-3′,5′-dihydroxyphenyl-β-oxy)ethylaminopropane Fumarate [(*R*,*S*)-2]. *R*,*S*-**2** was prepared from (*R*)-**8** and (*S*)-**11** according to procedure A to give 160 mg (38%). ^{1}H NMR (CD_3OD) δ 1.20 (d, 3H, J = 6.6 Hz), 2.62−2.71 (m, 1H), 2.98−3.20 (m, 3H), 3.30−3.42 (m, 2H), 4.73−4.81 (m, 1H), 6.21 (m, 2H), 3.35 (m, 2H), 6.71 (s, 0.5H, fumarate), 6.56−6.89 (m, 2H), 7.11−7.19 (m, 2H); ^{13}C NMR (CD_3OD) δ 15.6, 38.5, 51.8, 54.5, 55.9, 69.7, 102.1, 104.1, 114.1, 128.5, 130.2, 136.0, 143.8, 158.8, 159.1; UV (MeOH) λ_{max} 277 nm (ε 4100), 224 (21 400), 203 (50 600); MS (ESI+) *m*/*z* (rel) 318 (100, M + H); $[\alpha]_D$ = −7.2° (*c* 1.5, MeOH); HPLC (a) 70/30/0.05, 1.00 mL/min, 282 nm, t_R 1.40 min, 99% pure; (b) 50/50/0.05, 2.0 mL/min, 276 nm, t_R 1.51 min, 96.1% pure.

(*S*,*R*)-(+)-1-*p*-Methoxyphenyl-2-(β-3′,5′-dihydroxyphenyl-β-oxy)ethylaminopropane Fumarate [(*S*,*R*)-2]. *S*,*R*-**2** was prepared from (*S*)-**8** and (*R*)-**11**, according to procedure A to give 200 mg (51%). ^{1}H NMR (CD_3OD) δ 1.12 (d, 3H, J = 6.0 Hz), 2.58−3.13 (m, 5H), 3.77 (s, 3H), 4.62 (dd, 1H, J = 3.6, 9.0 Hz), 6.15 (m, 1H), 6.30 (d, 2H, J = 1.8 Hz), 6.85 (d, 2H, J = 8.7 Hz), 7.11 (d, 2H, J = 8.7 Hz); ^{13}C NMR (CD_3OD) δ 18.2, 41.4, 54.1, 55.7, 56.5, 64.7, 103.0, 105.3, 115.1, 130.7, 131.3, 145.9, 159.8, 160.0; UV (MeOH) λ_{max} 277 nm (ε 3150), 224 (3310), 205 (30 600); MS (ESI+) *m*/*z* (rel) 318 (100, M + H); $[\alpha]_D$ = +14.1° (*c* 0.95, MeOH); HPLC (a) 70/30/0.05, 1.00 mL/min, 282 nm, t_R 1.42 min, 97.7% pure; (b) 50/50/0.05, 2.0 mL/min, 276 nm, t_R 1.52 min, 97.8% pure.

(*R*,*R*)-(−)-5-{2-[2-(4-Aminophenyl)-1-methylethylamino]-1-hydroxyethyl}-1,3-benzenediol Fumarate [(*R*,*R*)-3]. *R*,*R*-**3** was prepared from (*R*)-**8** and (*R*)-**12** according to procedure A to give 88 mg (42%). ^{1}H NMR (CD_3OD) δ 1.23 (m, 3H), 2.70−3.24 (m, 4H), 3.54 (m, 1H), 4.84 (dd, 1H, J = 3.3, 9.6 Hz), 6.23 (t, 1H, J = 2.4 Hz), 6.38 (d, 2H, J = 2.1 Hz), 6.75 (s, 2H, fumarate), 7.35 (dd, 4H, J = 8.1, 21.0 Hz); ^{13}C (CD_3OD) δ 15.5, 39.6, 52.7, 56.6, 70.3, 103.4, 105.3, 123.8, 132.0, 132.1, 135.2, 137.5, 144.7, 160.0, 168.1; UV (MeOH) λ_{max} 284 nm (ε 1520), 206 (21 700); MS (ESI+) *m*/*z* (rel) 303 (100, M + H); $[\alpha]_D$ = −6.8° (*c* 1.0, MeOH); HPLC (a) 80/20/0.05, 0.70 mL/min, 276 nm, t_R 2.07 min, 95.5% pure; (b) 50/50/0.05, 1.0 mL/min, 282 nm, t_R 2.60, 97.16% pure.

(*S*,*S*)-(+)-5-{2-[2-(4-Aminophenyl)-1-methylethylamino]-1-hydroxyethyl}-1,3-benzenediol Fumarate [(*S*,*S*)-3]. *S*,*S*-**3** was prepared from (*S*)-**8** and (*S*)-**12** according to procedure A to give 56 mg (25%). ^{1}H NMR (CD_3OD) δ 1.23 (m, 3H), 2.62−3.27 (m, 4H), 3.55 (m, 1H), 4.74−4.88 (m, 1H), 6.22 (t, 1H, J = 1.8 Hz), 6.37 (d, 2H, J = 2.4 Hz), 6.75 (s, 2H, fumarate), 7.32 (dd, 4H, J = 8.7, 25.8 Hz); ^{13}C NMR (CD_3OD) δ 15.5, 39.6, 52.5, 56.7, 70.7, 103.4, 105.3, 123.3, 131.8, 132.0, 135.2, 136.9, 144.7, 160.0, 168.1; UV (MeOH) λ_{max} 284 nm (ε 1720), 207 (28 400); MS (ESI+) *m*/*z* (rel) 303 (100, M + H), 329 (20); $[\alpha]_D$ = +11.1° (*c* 0.50, MeOH); HPLC (a) 80/20/0.05, 0.7 mL/min, 276 nm, t_R 2.01 min, <99% pure; (b) 50/50/0.05, 1.0 mL/min, 282 nm, t_R 2.50 min, 99.4% pure.

(*R*,*S*)-(−)-5-{2-[2-(4-Aminophenyl)-1-methylethylamino]-1-hydroxyethyl}-1,3-benzenediol Fumarate [(*R*,*S*)-3]. *R*,*S*-**3** was prepared from (*R*)-**8** and (*S*)-**12** according to procedure A to give 72 mg (35%). ^{1}H NMR (CD_3OD) δ 1.23 (m, 3H), 2.73−3.24 (m, 4H), 3.51 (m, 1H), 4.80 (dd, 1H, J = 2.7, 9.6 Hz), 6.22 (t, 1H, J = 2.1 Hz), 6.36 (d, 2H, J = 2.4 Hz), 6.75 (s, 2H, fumarate), 7.32 (dd, 4H, J = 8.4, 25.2 Hz); ^{13}C NMR (CD_3OD) δ 16.1, 39.12, 5.16, 56.9, 70.4, 103.4, 105.3, 123.4, 132.0, 132.0, 135.2, 136.8, 144.6, 160., 168.10; UV (MeOH) λ_{max} 284 nm (ε 1620), 205 (27 200); MS (ESI+) *m*/*z* (rel) 303 (100, M + H), 134 (14); $[\alpha]_D$ = −7.5° (*c* 0.50, MeOH); HPLC (a) 80/20/0.05, 0.7 mL/min, 276 nm, t_R 2.08 min, 95.0% pure; (b) 50/50/0.05, 1.0 mL/min, 282 nm, t_R 2.51 min, 97.4% pure.

(*S*,*R*)-(+)-5-{2-[2-(4-Aminophenyl)-1-methylethylamino]-1-hydroxyethyl}-1,3-benzenediol Fumarate [(*S*,*R*)-3]. *S*,*R*-**3** was prepared from (*S*)-**8** and (*R*)-**12** according to procedure A to give 93 mg (42%). ^{1}H NMR (CD_3OD) δ 1.23 (d, 3H, J = 6.3 Hz), 2.70−3.78 (m, 4H), 3.42−3.62 (m, 1H), 4.80 (dd, 1H, J = 3.0, 9.9 Hz), 6.22 (t, 1H, J = 2.1 Hz), 6.37 (d, 2H, J = 2.1 Hz), 6.75 (s, 2H, fumarate), 7.33 (dd, 4H, J = 8.4, 26.7 Hz); ^{13}C NMR (CD_3OD) δ 16.2, 39.1, 52.6, 56.9, 70.5, 103.4, 105.3, 123.5, 132.1, 133.7, 135.2, 137.1, 144.7, 160.0, 168.1; UV (MeOH) λ_{max} 284 nm (ε 8230), 207 (100 000); MS (ESI+) *m*/*z* (rel) 303 (100, M + H), 134 (18); $[\alpha]_D$ = +11.4° (*c* 0.50, MeOH); HPLC (a) 70/30/0.05, 1.00 mL/min, 280 nm, t_R 1.45 min, 99% pure; (b) 50/50/0.05, 1.0 mL/min, 282 nm, t_R 2.63 min, 95.33% pure.

(*R*,*R*)-(−)-5-[1-Hydroxy-2-(1-methyl-2-phenylethylamino)ethyl]-1,3-benzenediol Fumarate [(*R*,*R*)-4]. *R*,*R*-**4** was prepared from (*R*)-**8** and (*R*)-**13** according to procedure A to give 92 mg (26%). ^{1}H NMR (CD_3OD) δ 1.22 (m, 3H), 2.68−3.28 (m, 2H), 3.10−3.28 (m, 2H), 3.53 (br-m, 1H), 4.75−4.80 (m, 1H), 6.24 (t, 1H, J = 2.4 Hz), 6.38 (d, 2H, J = 2.1 Hz), 6.75 (s, 1H, fumarate), 7.22−7.33 (m, 5H); ^{13}C NMR (CD_3OD) δ 15.5, 40.3, 56.9, 70.2, 103.4, 105.3, 128.3, 129.9, 130.3, 135.2, 137.3, 144.6, 144.6, 159.9, 168.1; UV (MeOH) λ_{max} 277 nm (ε 926), 204 (18 700); MS (APCI+) *m*/*z* 288 (100, M + H); $[\alpha]_D$ = −21.2° (*c* 0.85, MeOH); HPLC (a) 50/50/0.05, 1.00 mL/min, 282 nm; t_R 1.73 min; 99% pure; (b) 50/50/0.05, 2.0 mL/min, 276 nm, t_R 1.46 min, 97.5% pure.

(*S*,*S*)-(+)-5-[1-Hydroxy-2-(1-methyl-2-phenylethylamino)ethyl]-1,3-benzenediol Fumarate [(*S*,*S*)-4]. *S*,*S*-**4** was prepared from (*S*)-**8** and (*S*)-**13** according to procedure A to give 184 mg (51%). ^{1}H NMR (CD_3OD) δ 1.21 (m, 3H), 2.70−3.13 (m, 2H), 3.15−3.23 (m, 2H), 3.54 (br m, 1H), 4.79−4.86 (m, 1H), 6.24 (t, 1H, J = 2.1 Hz), 6.39 (t, 2H, J = 2.7 Hz), 6.76 (s, 1H, fumarate), 7.22−7.32 (m, 5H); ^{13}C NMR (CD_3OD) δ 15.5, 40.3, 56.9, 70.2, 103.4, 105.3, 128.3, 129.9, 130.3, 135.1, 137.3, 144.6, 144.6, 159.9, 168.1; UV (MeOH) λ_{max} 278 nm (ε 1510), 207 (26 600); MS (APCI+) *m*/*z* 288 (100, M + H); $[\alpha]_D$ = +19.3° (*c* 0.90, MeOH); HPLC (a) 50/50/0.05, 1.00 mL/min, 282 nm, t_R 1.49 min; 98.4% pure; (b) 50/50/0.05, 2.0 mL/min, 276 nm, t_R 1.35 min, 99% pure.

(*R*,*S*)-(−)-5-[1-Hydroxy-2-(1-methyl-2-phenylethylamino)ethyl]-1,3-benzenediol Fumarate [(*R*,*S*)-4]. *R*,*S*-**4** was prepared from (*R*)-**8** and (*S*)-**13** according to procedure A to give 170 mg (45%). ^{1}H NMR (CD_3OD) δ 1.22 (m, 3H), 2.68−3.28 (m, 2H), 3.13−3.28 (m, 2H), 3.53 (br m, 1H), 4.76−4.80 (m, 1H), 6.23 (t, 1H, J = 2.1 Hz), 6.37 (t, 2H, J = 3.0 Hz), 6.75 (s, 1H, fumarate), 7.24−7.37 (m, 5H); ^{13}C NMR (CD_3OD) δ 16.3, 24.2, 39.8, 57.2, 70.5, 103.4, 105.3, 128.4, 130.0, 130.4, 135.2, 137.4, 144.6, 160.1; UV (MeOH) λ_{max} 278 nm (ε 1110), 205 (31 000); MS (APCI+) *m*/*z* (rel) 288 (100, M + H); $[\alpha]_D$ = −6.9° (*c* 0.85, MeOH); HPLC (a) 50/50/0.05, 1.00 mL/min, 282 nm, t_R 1.53 min, 99% pure; (b) 50/50/0.05, 2.0 mL/min, 276 nm, t_R 1.46 min, 98.5% pure.

(*S*,*R*)-(+)-5-[1-Hydroxy-2-(1-methyl-2-phenylethylamino)ethyl]-1,3-benzenediol Fumarate [(*S*,*R*)-4]. *S*,*R*-**4** was prepared from (*S*)-**8** and (*R*)-**13** according to procedure A to give 212 mg (59%).

^{1}H NMR (CD_3OD) δ 1.22 (m, 3H), 2.72 (dd, 1H J = 10.2, 13.2 Hz), 3.11 (dd, 1H, J = 10.2, 12.6 Hz), 3.18−3.27 (m, 2H), 3.48−3.61 (m, 1H), 4.83 (dd, 1H, J = 3.3, 9.9 Hz), 6.22 (t, 1H, J = 2.4 Hz), 6.36 (d, 2H, J = 2.4 Hz), 6.75 (s, 1H, fumarate), 7.24−7.37 (m, 5H); ^{13}C NMR (CD_3OD) δ 16.3, 24.2, 39.8, 57.2, 70.5, 103.4, 105.3, 128.4, 130.0, 130.4, 135.2, 137.4, 144.6, 160.1; UV (MeOH) λ_{max} 278 nm (ϵ 1680), 206 (35 500); MS (APCI+) m/z (rel) 288 (100, M + H), 270 (19, M−OH); $[\alpha]_D$ = +9.1° (c 1.1, MeOH); HPLC (a) 50/50/0.05, 1.00 mL/min, 282 nm, t_R 1.51 min, 99% pure; (b) 50/50/0.05, 2.0 mL/min, 276 nm, t_R 1.43 min, 99% pure.

(*R*,*R*)-(−)-5-{1-hydroxy-2-[1-methyl-2-(1-naphthyl)ethylamino]ethyl}-1,3-benzenediol Fumarate [(*R*,*R*)-5]. *R*,*R*-**5** was prepared from (*R*)-**8** and (*R*)-**14** according to procedure A to give 135 mg (46%). ^{1}H NMR (CD_3OD) δ 1.18−1.23 (m, 3H), 3.16−3.34 (m,1H, 2H), 3.69−3.74 (m, 2H), 4.78−4.80 (m, 1H), 6.23 (t, 1H, J = 2.4 Hz), 6.38 (m, 2H), 7.41−7.61 (m, 4H), 7.83 (d, 1H, J = 7.5 Hz), 7.90 (d, 1H, J = 7.8 Hz), 8.10 (m, 1H); ^{13}C NMR (CD_3OD) δ 16.2, 37.2, 54.5, 56.1, 70.3, 103.4, 105.3, 124.3, 126.5, 127.0, 127.7, 129.3, 130.1, 133.2, 135.2, 135.6, 144.7, 160.1, 168.2; UV (MeOH) λ_{max} 282 nm (ϵ 5860), 224 (50 900), 208 (35 500); MS (APCI+) m/z (rel) 338 (100, M + H), 169 (15, fragment); $[\alpha]_D$ = −20.4 (c 0.50, MeOH); HPLC (a) 60/40/0.05, 1.00 mL/min, 282 nm, t_R 2.08 min, 95.7% pure; (b) 50/50/0.05, 1.5 mL/min, 282 nm, t_R 2.20 min, 99% pure.

(*S*,*S*)-(+)-5-{1-Hydroxy-2-[1-methyl-2-(1-naphthyl)ethylamino]ethyl}-1,3-benzenediol fumarate [(*S*,*S*)-5]. *S*,*S*-**5** was prepared from (*S*)-**8** and (*S*)-**14** according to procedure A to give 118 mg (40%). ^{1}H NMR (CD_3OD) δ 1.13−1.17 (m, 3H), 3.14−3.26 (m, 1H, 2H), 3.61−3.76 (m, 2H), 4.44−4.75 (m, 1H), 6.18 (t, 1H, J = 2.4 Hz), 6.33 (m, 2H), 7.36−7.52 (m, 4H), 7.77 (dd, 1H, J = 1.8, 7.5 Hz), 7.84 (d, 1H, J = 8.1 Hz), 8.04 (t, 1H, J = 8.4 Hz); ^{13}C NMR (CD_3OD) δ 16.1, 37.1, 54.4, 56.0, 70.3, 103.3, 105.3, 124.3, 126.5, 127.0, 127.7, 129.2, 130.0, 133.2, 135.2, 135.7, 144.5, 160.0, 168.1; UV (MeOH) λ_{max} 282 nm (ϵ 6210), 223 (56 400), 208 (42 700); MS (APCI+) m/z (rel) 338 (100, M + H), 169 (8, fragment); $[\alpha]_D$ = +20.0° (c 1.1% MeOH); HPLC (a) 60/40/0.05, 1.00 mL/min, 282 nm, t_R 2.35 min, 98.9% pure; (b) 50/50/0.05, 1.5 mL/min, 282 nm, t_R 2.26 min, 97.2% pure

(*R*,*S*)-(−)-5-{1-Hydroxy-2-[1-methyl-2-(1-naphthyl)ethylamino]ethyl}-1,3-benzenediol Fumarate [(*R*,*S*)-5]. *R*,*S*-**5** was prepared from (*R*)-**8** and (*S*)-**14** according to procedure A to give 114 mg (39%). ^{1}H NMR (CD_3OD) δ 1.08−1.11 (m, 3H), 3.02−3.24 (m, 1H, 2H), 3.54−3.68 (m, 2H), 4.45−4.75 (m, 1H), 6.11 (t, 1H, J = 1.8 Hz), 6.26 (m, 2H), 6.63 (s, 2H fumarate), 7.28−7.48 (m, 4H), 7.70 (d, 1H, J = 7.5 Hz), 7.77 (d, 1H, J = 7.8 Hz), 7.97 (t, 1H, J = 7.8 Hz); ^{13}C NMR (CD_3OD) δ 16.0, 37.1, 52.5, 56.0, 70.4, 103.4, 105.3, 124.4, 126.5, 127.0, 127.6, 129.2, 130.1, 133.1, 135.2, 135.5, 144.7, 159.9, 168.2; UV (MeOH) λ_{max} 281 nm (ϵ 12 600), 224 (61 900), 204 (47 200); MS (APCI+) m/z (rel) 338 (100, M + H), 190 (15, fragment); $[\alpha]_D$ = −11.3° (c 0.85, MeOH); HPLC (a) 60/40/0.05, 1.00 mL/min, 282 nm, t_r 2.30 min, 98.6% pure; (b) 50/50/0.05, 1.5 mL/min, 282 nm, t_R 2.36 min, 99% pure.

(*S*,*R*)-(+)-5-{1-Hydroxy-2-[1-methyl-2-(1-naphthyl)ethylamino]ethyl}-1,3-benzenediol Fumarate [(*S*,*R*)-5]. *S*,*R*-**5** was prepared from (*S*)-**8** and (*R*)-**14** according to procedure A to give 123 mg (42%). ^{1}H NMR (CD_3OD) δ 1.18−1.22 (m, 3H), 3.10−3.28 (m, 1H, 2H), 3.69−3.78 (m, 2H), 4.45−4.75 (m, 1H), 6.23 (t, 1H, J = 2.1 Hz), 6.39 (m, 2H), 6.73 (s, 2H fumarate), 7.39−7.59 (m, 4H), 7.80 (d, 1H, J = 7.5 Hz), 7.88 (d, 1H, J = 7.8 Hz), 8.01 (t, 1H, J = 9.0 Hz); ^{13}C NMR (CD_3OD) δ 16.4, 37.4, 52.5, 56.2, 70.6, 103.4, 105.3, 124.4, 126.5, 127.0, 129.3, 130.1, 133.1, 133.4, 135.6, 136.3, 144.8, 160.0, 171.4; UV (MeOH) λ_{max} 282 nm (ϵ 7740), 224 (70 900), 206 (55 800); MS (ESI+) m/z (rel) 338 (100, M + H); $[\alpha]_D$ = +15.5 (c 1.0, MeOH); HPLC (a) 60/40/0.05, 1.0 mL/min, 282 nm, t_R 1.95, 95.7% pure; (b) 50/50/0.05, 1.5 mL/min, 282 nm, t_R 2.29 min, 95.7% pure

(*R*,*R*)-(−)-5-[1-Hydroxy-2-(1-methylhexylamino)ethyl]-1,3-benzenediol Fumarate [(*R*,*R*)-6]. *R*,*R*-**6** was prepared from (*R*)-**8** and (*R*)-**15** according to procedure A to give 45 mg (29%). ^{1}H NMR (CD_3OD) δ 0.920 (t, 3H, J = 6.9 Hz), 1.30 (d, 3H, J = 6.9 Hz), 1.29−1.64 (m, 8H), 3.01−3.18 (m, 2H), 3.14−3.30 (m, 1H), 4.80 (dd, 1H, J = 3.3, 9.6 Hz), 6.22 (t, 1H, J = 2.1 Hz), 6.36 (d, 2H, J = 2.4 Hz), 6.75 (s, 1H, fumarate); ^{13}C NMR (CD_3OD) δ 14.3, 16.0, 23.5, 26.2, 32.6, 34.2, 52.1, 55.7, 70.2, 103.3, 105.3, 135.2, 144.7, 160.0, 168.0; UV (MeOH) λ_{max} 278 nm (ϵ 931), 203 nm (20 100); MS (ESI+) m/z (rel) 268 (100, M + H); $[\alpha]_D$ = −8.8° (c 1.1, MeOH); HPLC (c) 70/30/0.1, 1.0 mL/min, 276 nm, t_R 2.18 min, 96.6% pure; (b) 50/50/0.05, 1.0 mL/min, 279 nm, t_R 2.06 min, 98.9% pure.

(*S*,*S*)-(+)-5-[1-Hydroxy-2-(1-methylhexylamino)ethyl]-1,3-benzenediol Fumarate [(*S*,*S*)-6]. *S*,*S*-**6** was prepared from (*S*)-**8** and (*S*)-**15** according to procedure A to give 96 mg (43%). ^{1}H NMR (CD_3OD) δ 0.923 (t, 3H, J = 6.6 Hz); 1.31 (d, 3H, J = 6.6 Hz), 1.26−1.84 (m, 8H), 2.01−3.18 (m, 2H), 3.14−3.30 (m, 1H), 4.81 (dd, 1H, J = 3.3, 9.6 Hz), 6.23 (t, 1H, J = 2.4 Hz), 6.39 (d, 2H, J = 2.1 Hz), 6.76 (s, 1H, fumarate): ^{13}C NMR (CD_3OD) δ 14.2, 16.0, 23.4, 26.3, 32.6, 34.1, 52.1, 55.8, 70.2, 103.4, 105.3, 135.2, 144.7, 159.9, 168.2; UV (MeOH) λ_{max} 278 nm (ϵ 1340), 203 (28 800); MS (APCI+) m/z (rel) 268 (100, M + H); $[\alpha]_D$ = +10.8° (c 0.50, MeOH); HPLC (c) 70/30/0.1, 1.0 mL/min, 276 nm, t_R 2.16 min, 97.0% pure; (b) 50/50/0.05, 1.0 mL/min, 279 nm, t_R 2.11 min, 99% pure.

(*R*,*S*)-(−)-5-[1-Hydroxy-2-(1-methylhexylamino)ethyl]-1,3-benzenediol Fumarate [(*R*,*S*)-6]. *R*,*S*-**6** was prepared from (*R*)-**8** and (*S*)-**15** according to procedure A to give 83 mg (38%). ^{1}H NMR (CD_3OD) δ 0.924 (m, 3H), 1.32 (d, 3H, J = 6.6 Hz), 1.26−1.84 (m, 8H), 2.98−3.20 (m, 2H), 3.32−3.22 (m, 1H), 4.78 (dd, 1H, J = 3.0, 9.9 Hz), 6.23 (t, 1H, J = 2.1 Hz), 6.37 (d, 2H, J = 1.8 Hz), 6.76 (s, 1H, fumarate); ^{13}C NMR (CD_3OD) δ 14.2, 16.4, 23.4, 26.2, 32.6, 33.5, 52.2, 56.0, 70.4, 103.4, 105.3, 135.2, 144.7, 160.0, 168.1; UV (MeOH) λ_{max} 276 nm (ϵ 2770), 203 (35 900); MS (APCI+) m/z (rel) 268 (100, M + H); $[\alpha]_D$ = −15.9° (c 0.70, MeOH); HPLC (c) 70/30/0.1, 1.0 mL/min, 276 nm, t_R 2.16 min, 97.0% pure; (b) 50/50/0.05, 1.0 mL/min, 279 nm, t_R 2.07 min, 96.2% pure.

(*S*,*R*)-(+)-5-[1-Hydroxy-2-(1-methylhexylamino)ethyl]-1,3-benzenediol Fumarate [(*S*,*R*)-6]. *S*,*R*-**6** was prepared from (*S*)-**8** and (*R*)-**15** according to procedure A to give 81 mg (38%). ^{1}H NMR (CD_3OD) δ 0.920 (t, 3H, J = 6.3 Hz), 1.32 (d, 3H, J = 6.9 Hz), 1.30−1.77 (m, 8H), 2.99−3.17 (m, 2H), 3.23−3.26 (m, 1H), 4.76 (dd, 1H, J = 3.0, 9.6 Hz), 6.22 (t, 1H, J = 2.4 Hz), 6.36 (d, 2H, J = 2.1 Hz), 6.75 (s, 1H, fumarate); ^{13}C NMR (CD_3OD) δ 14.2, 16.5, 23.5, 26.2, 32.6, 39.5, 52.2, 56.0, 70.4, 103.4, 105.3, 135.2, 144.7, 160.0, 168.0; UV (MeOH) λ_{max} 278 nm (ϵ 1440), 204 (29 900); MS (APCI+) m/z (rel) 268 (100, M + H); $[\alpha]_D$ = +12.7° (c 1.0, MeOH); HPLC (c) 70/30/0.1, 1.0 mL/min, 276 nm, t_R 2.16 min, 99% pure; (b) 50/50/0.05, 1.0 mL/min, 279 nm, t_R 2.02 min, 95.7% pure.

(*R*)-(−)-5-(1-Hydroxy-2-phenethylaminoethyl)-1,3-benzenediol Fumarate [(*R*)-7]. *R*-**7** was prepared from (*R*)-**8** and **28** (Aldrich) to give 37 mg (15%). ^{1}H NMR (CD_3OD) δ 2.94−3.23 (m, 6H), 4.73 (dd, 1H, J = 3.3, 9.9 Hz), 6.15 (t, 1H, J = 2.4 Hz), 6.29 (d, 2H, J = 1.8 Hz), 7.19−7.28 (m, 5H), 6.69 (s, 1H); UV (MeOH) λ_{max} 278 nm (ϵ 1360), 205 (32 600); MS (APCI+) m/z (rel) 274 (100, M + H); $[\alpha]_D$ = −13.0° (c 1.0, MeOH); HPLC (a) 80/20/0.05, 1.00 mL/min, 282 nm, t_R 1.47 min, 96.7% pure; (b) 50/50/0.05, 1.0 mL/min, 272 nm, t_R 2.78 min, 95.1% pure.

(*S*)-(+)-5-(1-Hydroxy-2-phenethylaminoethyl)-1,3-benzenediol Fumarate [(*S*)-7]. *S*-**7** was prepared from (*S*)-**8** and **28** (Aldrich) to give 51 mg (17%). ^{1}H NMR (CD_3OD) δ 2.87−3.21 (m, 6H), 4.68 (dd, 1H, J = 3.6, 9.9 Hz), 6.10 (t, 1H, J = 2.4 Hz), 6.24 (d, 2H, J = 2.1 Hz), 6.63 (s, 1H), 7.12−7.21 (m, 5H); UV (MeOH) λ_{max} 278 nm (ϵ 1280), 204 (33 700); MS (APCI+) m/z (rel) 274 (100, M + H); $[\alpha]_D$ = +14.64° (c 1.1, MeOH); HPLC (a) 80/20/0.05, 1.00 mL/min, 282 nm, t_R 1.47 min, 98.6% pure; (b) 50/50/0.05, 1.0 mL/min, 272 nm, t_R 2.74 min, 98.8% pure.

Acknowledgment. This work was supported in part by funds from the National Institute on Aging, Intramural Research Program, NIA Contract N01-AG-3-1009 and the Foundation for Polish Science (FOCUS 4/2006 programme). K.J. would like to acknowledge Professor D. Matosiuk from the Department

of Synthesis and Chemical Technology of Pharmaceutical Substance, Medical University of Lublin, for letting him use the QSAR software.

References

(1) O'Donnell, S. R. A selective β-adrenoceptor stimulant (Th1165a) related to orciprenaline. *Eur. J. Pharmacol*. **1970**, *12*, 35−43.
(2) Heel, R. C.; Brogden, R. C.; Speight, T. M.; Avery, G. S. Fenerotol: A review of its pharmacological properties and therapeutic efficacy in asthma. *Drugs* **1978**, *15*, 3−32.
(3) Xiao, R.-P.; Zhang, S.-J.; Chakir, K.; Avdonin, P.; Zhu, W.; Bond, R. A.; Balke, C. W.; Lakatta, E. G.; Cheng, H. Enhanced G_i signaling selectively negates β_2-adrenergic receptor (AR)─But not β_1AR-mediated positive inotropic effect in myocytes from failing rat hearts. *Circulation* **2003**, *108*, 1633−1639.
(4) Xiao, R.-P.; Zhu, W.; Zheng, M.; Chakir, K.; Bond, R.; Lakatta, E. G.; Cheng, H. Subtype-specific β-adrenoceptor signaling pathways in the heart and their potential clinical implications. *Trends Pharmacol. Sci*. **2004**, *25*, 358−365.
(5) Kaiser, G.; Wiemer, G.; Kremer, G.; Dietz, J.; Palm, D. Identification and quantification of β-adrenoceptor sites in red blood cells from rats. *Naunyn-Schmiedeberg's Arch. Pharmacol.* **1978**, *305*, 41−50.
(6) Beigi, F.; Bertucci, C.; Zhu, W.; Chakier, K.; Wainer, I. W.; Xiao, R.-P.; Abernethy, D. A. Enantioselective separation and online affinity chromatographic characterization of *R*,*R*- and *S*,*S*-fenoterol. *Chirality* **2006**, *18*, 822−827.
(7) Trofast, J.; Österberg, K.; Källström, B.-R.; Waldek, B. Steric aspects of agonism and antagonism at β-adrenoceptors: Synthesis of and pharmacological experiments with the enantiomers of formoterol and their diastereomers. *Chirality* **1991**, *3*, 443−450.
(8) Pauwels, P. J.; Van Gompel, P.; Leysen, J. E. Human β_1- and β_2-adrenergic receptor binding and mediated accumulation of cAMP in transfected Chinese hamster ovary cells. *Biochem. Pharmacol*. **1991**, *42*, 1683−1689.
(9) Cheng,Y. C.; Prusoff, W. H. Relationship between the inhibition constant (K_i) and the concentration of inhibitor which causes 50 percent inhibition (I_{50}) of an enzymatic reaction. *Biochem. Pharmacol.* **1973**, *22*, 3099−3108.
(10) Eimerl, S.; Schramm, M.; Lok, S.; Goodman, M.; Khan, M.; Melmon, K. The four stereoisomers of a high potency congener of isoproterenol: Biological activity and the relationship between the native and the chemically inserted asymmetric carbon. *Biochem. Pharmacol.* **1987**, *36*, 3523−3527.
(11) Wieland, K.; Zuurmond, H. M.; Krasel, C.; Ijzerman, A. D. P.; Lohse, M. J. Involvement of Asn-293 in stereospecific agonist recognition and in activation of the β_2-adrenergic receptor. *Proc. Natl. Acad. Sci. U.S.A.* **1996**, *93*, 9276−9281.
(12) Kikkawa, H.; Isogaya, M.; Nagao, T.; Kurose, H. The role of the seventh transmembrane region in high affinity binding of a β_2-selective agonist TA-2005. *Mol. Pharmacol.* **1998**, *53*, 128−134.
(13) Zuurmond, H. M.; Hessling, J.; Blüml, K.; Lohse, M.; Ijzerman, A. P. Study of interaction between agonists and Asn293 in helix VI of human β_2-adrenergic receptor. *Mol. Pharmacol.* **1999**, *56*, 909−916.
(14) Schirrmacher, E.; Schirrmacher, R.; Thews, O.; Dillenburg, W.; Helisch, A.; Wessler, I.; Buhl, R.; Hohnemann, S.; Buchholz, H. G.; Bartenstein, P.; Machulla, H. J.; Rosch, F. Synthesis and preliminary evaluation of (R,R) (S,S) 5-(2-(2-[4-(2-[(18)F] fluoroethoxy)phenyl]-1-methylethylamino)-1-hydroxyethl)-benzene-1,3-diol ([(18)F]FEFE) for the in vivo visualization and quantification of the beta2-adrenergic receptor status in lung. *Bioorg. Med. Chem. Lett.* **2003**, *13*, 2687−2692.
(15) Beer, M.; Richardson, A.; Poat, J.; Iversen L. L.; Stahl, S. M. *In vitro* selectivity of agonists and antagonists for beta$_1$- and beta$_2$-adrenoceptor subtypes in rat brain. *Biochem. Pharmacol.* **1988**, *37*, 1145−1151.
(16) Cramer, R. D., III; Patterson, D. E.; Bunch, J. D. Comparative molecular field analysis (CoMFA). 1. Effect of shape on binding of steroids to carrier proteins. *J. Am. Chem. Soc.* **1988**, *110*, 5959−5967.
(17) Kubinyi, H. Comparative Molecular Field Analysis (COMFA). *Encyclopedia of Computational Chemistry*; John Wiley & Sons, Ltd.: New York, 1998; http://www.wiley.com//legacy/wileychi/ecc/.
(18) Kontoyianni, M.; DeWeese, C.; Penzotti, J. E.; Lybrand, T. P. Three-dimensional models for agonist and antagonist complexes with β_2 adrenergic receptor. *J. Med. Chem.* **1996**, *39*, 4406−4420.
(19) Furse, K. E.; Lybrand, T. P. Three-dimensional models for β-adrenergic receptor complexes with agonists and antagonists. *J. Med. Chem*. **2003**, *46*, 4450−4462.
(20) Swaminath, G.; Xiang, Y.; Lee, T. W.; Steenhuis, J.; Parnot, C.; Kobilka, B. K. Sequential binding of agonists to the β_2 adrenoceptor. *J. Biol. Chem*. **2004**, *279*, 686−691.
(21) Levitt, M.; Perutz, M. F. Aromatic rings act as hydrogen bond acceptors. *J. Mol. Biol.* **1988**, *201*, 751−754.
(22) Kobilka, B. Agonist binding: A multistep process. *Mol. Pharm.* **2004**, *65*, 1060−1062.
(23) Sokolov, V. I.; Zefirov, N. S. Enantioselectivity in two-point binding: Rocking tetrahedron model. *Dokl. Akad. Nauk SSSR* **1991**, *319*, 1382−1383.

JM070030D